Katholieke Universiteit Leuven

Departement Elektrotechniek

ESAT-SISTA/TR 2003-167

Adaptive feedback cancellation in hearing aids with linear prediction of the desired signal [1]

Ann Spriet[2], Ian Proudler[3] ,Marc Moonen[4] ,Jan Wouters[5]

Published in IEEE Trans. Signal Processing, vol. 53. no. 10, October 2005.

[1]This report is available by anonymous ftp from *ftp.esat.kuleuven.be* in the directory *pub/sista/spriet/reports/03-167.pdf*

[2]K.U.Leuven, Dept. of Electrical Engineering (ESAT), SISTA, Kasteelpark Arenberg 10, 3001 Leuven-Heverlee, Belgium, Tel. 32/16/32 18 99, Fax 32/16/32 19 70, WWW: *http://www.esat.kuleuven.be/sista*. E-mail: *ann.spriet@esat.kuleuven.be*. K.U.Leuven, Lab. Exp. ORL/ ENT-Dept., Kapucijnenvoer 33, 3000 Leuven, Belgium, Tel. 32/16/33 24 15, Fax 32/16/33 23 35, WWW: *http://www.kuleuven.ac.be/exporl/Lab/Default.htm*. Ann Spriet is a Research Assistant of the Katholieke Universiteit Leuven. This research was carried out at the ESAT laboratory and Lab. Exp. ORL of K.U. Leuven, in the frame of the Belgian Programme on Interuniversity Attraction Poles, initiated by the Belgian Federal Science Policy Office IUAP P5/22 (Dynamical Systems and Control: Computation, Identification and Modelling), the Concerted Research Action GOA-MEFISTO-666 (Mathematical Engineering for Information and Communication Systems Technology) of the Flemish Government, FWO Project nr. G.0233.01 (Signal processing and automatic patient fitting for advanced auditory prostheses), IWT project 020540 (Innovative Speech Processing Algorithms for Improved Performance of Cochlear Implants), IWT project 020476 (SMS4PA: Sound Management System for Public Address Systems) and was partially sponsored by QinetiQ. The scientific responsibility is assumed by its authors.

[3]QinetiQ Ltd., Malvern Technology Centre, St Andrews Road, Malvern, Worcestershire, WR14 3PS, UK. Tel: +44 (0) 1684 894228, Fax: +44 (0) 1684 896502, E-mail: *i.proudler@signal.qinetiq.com*.

[4]K.U.Leuven, Dept. of Electrical Engineering (ESAT), SISTA, Kasteelpark Arenberg 10, 3001 Heverlee, Belgium, Tel. 32/16/32 17 09, Fax 32/16/32 19 70, WWW: *http://www.esat.kuleuven.be/sista*. E-mail: *marc.moonen@esat.kuleuven.be*. Marc Moonen is a professor at the Katholieke Universiteit Leuven.

[5]K.U.Leuven, Lab. Exp. ORL, Dept. Neurowetenschappen, Kapucijnenvoer 33, 3000 Leuven, Belgium, Tel. 32/16/33 23 42, Fax 32/16/33 23 35, WWW: *http://www.kuleuven.ac.be/exporl/Lab/Default.htm* E-mail: *jan.wouters@uz.kuleuven.ac.be*. Jan Wouters is a professor at the Katholieke Universiteit Leuven.

Adaptive feedback cancellation in hearing aids with linear prediction of the desired signal

Ann Spriet*[1,2], *Student Member, IEEE,* Ian Proudler[3], Marc Moonen[1], *Member, IEEE,* Jan Wouters[2]

[1]ESAT/SCD-SISTA, K.U. Leuven

Kasteelpark Arenberg 10, B-3001 Leuven-Heverlee, Belgium

Tel.: +32 16 321795, Fax: +32 16 321970

E-mail: ann.spriet@esat.kuleuven.be; marc.moonen@esat.kuleuven.be

[2]Lab. Exp. ORL / ENT-Dept., K.U. Leuven

Kapucijnenvoer 33, B-3000 Leuven, Belgium

E-mail: jan.wouters@uz.kuleuven.ac.be

[3]QinetiQ Ltd., Malvern Technology Centre

St Andrews Road, Malvern, Worcestershire, WR 14 3 PS, United Kingdom

E-mail: i.proudler@signal.QinetiQ.com

Manuscript received April 5, 2003; revised August 23, 2004. This research was carried out at the ESAT laboratory and Lab. Exp. ORL of K.U. Leuven, in the frame of the Belgian Programme on Interuniversity Attraction Poles, initiated by the Belgian Federal Science Policy Office IUAP P5/22 ('Dynamical Systems and Control: Computation, Identification and Modelling'), the Concerted Research Action GOA-MEFISTO-666 (Mathematical Engineering for Information and Communication Systems Technology) of the Flemish Government, FWO Project nr. G.0233.01 (Signal processing and automatic patient fitting for advanced auditory prostheses), IWT project 020540 (Innovative Speech Processing Algorithms for Improved Performance of Cochlear Implants), IWT project 020476 (SMS4PA: Sound Management System for Public Address Systems) and was partially sponsored by QinetiQ. The scientific responsibility is assumed by its authors.The associate editor coordinating the review of this paper and approving it for publication was Prof. Steven Grant.

A. Spriet and M. Moonen are with the Katholieke Universiteit Leuven, Department of Electrical Engineering (ESAT-SCD), B-3001 Leuven, Belgium (e-mail: ann.spriet@esat.kuleuven.be, marc.moonen@esat.kuleuven.be).

A. Spriet and J. Wouters are with the Katholieke Universiteit Leuven, ENT-Department (Lab. Exp. ORL), B-3000 Leuven, Belgium (e-mail: jan.wouters@uz.kuleuven.ac.be).

I. Proudler is with QinetiQ Ltd, Malvern Technology Centre, Worcestershire, WR 14 3 PS, United Kingdom (e-mail: i.proudler@signal.qinetiq.com).

Abstract

The standard continuous adaptation feedback cancellation algorithm for feedback suppression in hearing aids suffers from a large model error or bias if the received sound signal is spectrally colored. To reduce the bias in the feedback path estimate, we propose adaptive feedback cancellation techniques that are based on a closed-loop identification of the feedback path as well as the (auto-regressive) modelling of the desired signal. In general, both models are not simultaneously identifiable in the closed-loop system at hand. We show that –under certain conditions, e.g., if a delay is inserted in the forward path– identification of both models is indeed possible. Two classes of adaptive procedures for identifying the desired signal model and the feedback path are derived: a two-channel identification method as well as a prediction error method. In contrast to the two-channel identification method, the prediction error method allows use of different adaptation schemes for the feedback path and for the desired signal model and hence, is found to be preferable for highly non-stationary sound signals. Simulation results demonstrate that the proposed techniques outperform the standard continuous adaptation algorithm, if the conditions for identifiability are satisfied.

Index Terms

Adaptive feedback cancellation, direct closed-loop identification, identifiability conditions, linear prediction, hearing aids

I. INTRODUCTION

Hearing aids try to compensate for the increased hearing threshold of hearing impaired people by amplifying the desired sound signal $x[k]$. However, signal leakage from the hearing aid loudspeaker into the microphone, referred to as acoustic feedback, limits the maximum amplification that can be used in a hearing aid without making it unstable. In many cases this maximum amplification is too small to compensate for the hearing loss. Therefore, feedback suppression algorithms are called for.

A promising solution for acoustic feedback is the use of a *feedback cancellation* algorithm, as illustrated in **Figure 1**. The signal processing path of the hearing aid, the so-called forward path, is denoted by $G(q)$; the acoustic feedback path between the loudspeaker and the microphone is denoted by $F(q)$. The loudspeaker and microphone signal are $u[k]$ and $y[k]$, respectively. The feedback canceller $\hat{F}_0(q)$ estimates the feedback signal $F(q)u[k]$[1] and subtracts it from the microphone signal $y[k]$, so that ideally, only the

[1]The notation will be defined at the end of this section but suffice it to say that $F(q)u[k]$ is the result of filtering the signal $u[k]$ with the filter $F(q)$.

desired signal $x[k]$ is processed by $G(q)$. Since the feedback path $F(q)$ can vary significantly depending on the acoustical environment [1]-[4], the feedback canceller must be adaptive.

Currently available *adaptive feedback cancellers* can be divided into two classes: algorithms with a continuous adaptation and algorithms with a *non-continuous adaptation* [5], [6]. The latter adapt the filter only when instability is detected or when the input signal level is low [7]-[9]. Due to the reactive, rather than proactive, adaptation, these systems may be objectionable. A *continuous adaptation* feedback canceller (CAF) continuously adapts the coefficients of the filter $\hat{F}(q)$, based on standard adaptive filtering (Wiener filtering) procedures. This is depicted in **Figure 1**. The filter $\hat{F}_0(q)$ in the feedback cancellation path is an initial estimate of $F(q)$. It is continuously replaced during adaptation by the estimate $\hat{F}(q)$. Because of the presence of $G(q)$, the desired signal $x[k]$ and the input $u[k]$ to the adaptive filter $\hat{F}(q)$ are correlated when $x[k]$ is spectrally colored, thereby causing a biased feedback path estimate $\hat{F}(q)$ [10]. The filter $\hat{F}(q)$ will then cancel the desired signal $x[k]$ as well as the feedback signal $F(q)u[k]$ leading to desired signal distortion.

In the literature, different solutions have been proposed to *reduce the bias* in case of spectrally colored input signals $x[k]$. Classical approaches include introducing signal decorrelating operations in the forward path or the cancellation path (such as delays or non-linearities) [10]-[13], adding a probe signal $r[k]$ to the loudspeaker input $u[k]$ [14], [15] and controlling the adaptation of the feedback canceller $\hat{F}(q)$, e.g., by means of constrained or bandlimited adaptation [16]-[19]. Generally, these techniques involve a trade off between desired signal cancellation on the one hand and tracking performance or sound quality on the other hand with the result that typically a significant residual bias still remains.

In [20]-[22], alternative solutions for the bias in the feedback path estimate have been presented that are based on closed-loop system identification [23], [24]. Depending on the assumptions that are made about the forward path, closed-loop identification methods can be classified as direct, indirect or joint input-output methods [23]. In contrast to the indirect and the joint input-output approach, the direct method requires neither assumptions about the forward path $G(q)$ (e.g., linear) nor the presence of a probe signal $r[k]$, making it an appealing approach for feedback cancellation. In [20], [21], an adaptive feedback cancellation technique based on the direct method of closed-loop identification and a *fixed* estimate of the desired signal model has been proposed. It has been shown that the bias of the feedback path estimate can be avoided if the desired signal $x[k]$ can be modelled as $H(q)w[k]$ where $w[k]$ is white noise, and the desired signal model $H(q)$ is inversely stable and known. In practice, the desired signal model $H(q)$ is unknown and highly time-varying so that it is desirable to estimate this model adaptively. In general though, the feedback path $F(q)$ and the desired signal model $H(q)$ are not both identifiable

in closed-loop, unless a probe signal $r[k]$ is inserted or non-linearities are added to $G(q)$ [21].

In this paper, we revise the conditions for identifiability of the feedback path and the desired signal model with the direct method of closed-loop identification. We show that not only inserting non-linearities or a probe signal, but also adding a small delay in the forward path $G(q)$ or in the cancellation path $\hat{F}(q)$ can render the system identifiable. In addition, adaptive feedback cancellation techniques based on direct closed-loop identification of the feedback path as well as the (autoregressive (AR)) modelling of the desired signal are developed with the aim of providing an unbiased feedback path estimate for an unknown desired signal $x[k]$. The paper is organized as follows. **Section II** reviews the concept of direct closed-loop identification of the feedback path $F(q)$ and the desired signal $H(q)$ with the prediction error method (PEM), as proposed in [21]. In **Section III**, we derive conditions under which minimizing the PEM cost function results in a unique and unbiased solution for both the feedback path $F(q)$ and the desired signal model $H(q)$. In **Section IV**, two classes of adaptive identification procedures for estimating the feedback path $F(q)$ and the desired signal model $H(q)$ are derived, namely, a two-channel adaptive feedback canceller (2-ch AFC) as well as a prediction error method based adaptive feedback canceller (PEM-AFC). In contrast to the 2-ch AFC method, the PEM-AFC allows use of different adaptation schemes for the feedback path and for the desired signal model and hence, is found to be preferable for highly non-stationary sound signals. Simulations in **Section V** demonstrate that the proposed algorithms outperform the standard CAF algorithm, when the conditions for identifiability are fulfilled and that for highly time-varying sound signals such as speech and music, the PEM-AFC offers the best performance.

Notation

The superscript T denotes matrix/vector transpose. The discrete-time index is denoted by k. The symbol q^{-1} denotes the discrete-time delay operator, i.e., $q^{-1}u[k] = u[k-1]$. A discrete-time filter with filter length L_F is represented as a polynomial $F(q)$ in q, i.e.,

$$F(q) \quad = \quad f_0 + f_1 q^{-1} + f_2 q^{-2} + \cdots + f_{L_F-1} q^{-L_F+1} \tag{1}$$

or, alternatively, by its coefficient vector $\mathbf{f} = \begin{bmatrix} f_0 & f_1 & \cdots & f_{L_F-1} \end{bmatrix}^T$. The filtering of $u[k]$ with $F(q)$ is then denoted as

$$F(q)u[k] \quad = \quad \mathbf{f}^T \mathbf{u}[k], \tag{2}$$

with $\mathbf{u}[k] = \begin{bmatrix} u[k] & u[k-1] & \cdots & u[k-L_F+1] \end{bmatrix}^T$. The filter $F(q,k)$ refers to a time-varying filter with coefficient vector $\mathbf{f}[k]$. The spectrum of $F(q)$ is denoted by $F(e^{j\omega})$ with $\omega \in [0, \pi]$ the normalized angular frequency.

II. DIRECT CLOSED-LOOP IDENTIFICATION OF THE FEEDBACK PATH

Figure 2 illustrates the concept of direct closed-loop identification of the feedback path $F(q)$ and signal model $H(q)$ with the prediction error method (PEM), as proposed by [20], [21]. The signal $r[k]$ is an optional probe signal that is independent of $x[k]$. Generally, $r[k]$ is a noise signal. We assume that $G(q)$ has a delay d_1 of at least one sample and that the desired signal $x[k] = H(q)w[k]$, where $w[k]$ is white noise and $H(q)$ is monic and inversely stable. In general, $x[k]$ is an audio signal (e.g., a speech segment). Many audio signals can be closely approximated as a low-order AR random process

$$x[k] = H(q)w[k] = \frac{1}{1 + q^{-1}P(q)}w[k], \tag{3}$$

where $w[k]$ is a white noise signal[2]. Then, the open-loop system $\{F(q),\ H(q)\}$ to be identified is described by

$$y[k] = F(q)u[k] + H(q)w[k]. \tag{4}$$

In closed-loop identification with the direct method, the open-loop system is identified based on $u[k]$ and $y[k]$, thereby ignoring the presence of the forward path $G(q)$. The filter $\hat{F}_0(q)$ in Figure 2 is an initial estimate of $F(q)$ such that the closed-loop system $\frac{G(q)}{1-G(q)(F(q)-\hat{F}_0(q))}$ is stable. It is typically replaced during identification by the estimate $\hat{F}(q)$. In this case, the data $u[k]$ and $y[k]$ depend on $\hat{F}(q)$.

A possible identification method for $\hat{F}(q)$ is the *prediction error method*. The PEM produces an estimate $\hat{F}(q)$ and $\hat{H}(q)$ of the feedback path $F(q)$ and the signal model $H(q)$, respectively, by minimizing the difference between the measured output $y[k]$ and the predicted output $\hat{y}[k]$, called the prediction error $e_p[k]$. The optimal one step ahead predictor of $y[k]$ with the model $\left\{\hat{F}(q),\ \hat{H}(q)\right\}$ equals [23], [24]

$$\hat{y}[k] = \hat{H}(q)^{-1}\hat{F}(q)u[k] + [1 - \hat{H}(q)^{-1}]y[k]. \tag{5}$$

Using (5), the prediction error $e_p[k] = y[k] - \hat{y}[k]$ can be written as

$$e_p[k] = \hat{H}(q)^{-1}[y[k] - \hat{F}(q)u[k]]. \tag{6}$$

A standard criterion for $\hat{F}(q)$ and $\hat{H}(q)$ is to minimize the time-average of squared prediction errors:

$$\frac{1}{N}\sum_{k=0}^{N-1} e_p^2[k]. \tag{7}$$

Since $\hat{F}(q)$ is multiplied by $\hat{H}(q)^{-1}$ in (6), the PEM cost function (7) is non-linear in $\hat{F}(q)$ and $\hat{H}^{-1}(q)$.

[2]Note that the white noise assumption is not satisfied for periodic signals such as voiced speech segments or music (cf. Section III-A). E.g., in the case of voiced speech segment, the excitation $w[k]$ is an impulse train [25].

In [20], [21], the desired signal model $H(q)$ is approximated by a *fixed* low-pass filter $\hat{H}(q)$, which represents the long-term average spectrum of speech. If $\hat{H}(q) = H(q)$ and $w[k]$ is white noise, minimizing (7) results in an *unbiased* feedback path estimate $\hat{F}(q) = F(q)$. In practice, however, $H(q)$ is unknown and time-varying. In addition, the accuracy of the feedback path estimate $\hat{F}(q)$ strongly depends on the quality of the estimate $\hat{H}(q)$ [21] so that it is desirable to estimate $H(q)$ adaptively. In general though, $H(q)$ and $F(q)$ are not simultaneously identifiable in closed-loop if the probe signal $r[k] = 0$, $G(q)$ is linear and the filter $\hat{F}_0(q)$ is fixed [21]. This implies that, besides the desired solution $\hat{F}(q) = F(q)$ and $\hat{H}(q) = H(q)$, alternative spurious solutions for $\hat{F}(q)$ and $\hat{H}(q)$ may exist. Hence, convergence of the adaptive filters $\hat{F}(q)$ and $\hat{H}(q)$ towards the desired solution is not guaranteed. The unidentifiability is caused by the forward path $G(q)$, which induces a linear relationship between the loudspeaker signal $u[k]$ and the microphone signal $y[k]$. In Section III, we revise the conditions for identifiability of $F(q)$ and $H(q)$. We demonstrate that besides inserting a probe signal or adding non-linearities also adding a delay in the forward path $G(q)$ or in the cancellation path can render the system identifiable.

III. Conditions for identifiability

In this section, we derive conditions under which both the inverse desired signal model $H^{-1}(q)$ and the feedback path $F(q)$ can be identified by minimizing the PEM cost function (7). To derive the conditions for identifiability, we convert the non-linear PEM cost function (7) into a linear cost function by replacing $\hat{H}^{-1}(q)$ by $A(q)$ and the product $-\hat{H}^{-1}(q)\hat{F}(q)$ by $B(q)$, where the adaptive FIR filters $A(q)$ and $B(q)$ have coefficient vectors $\mathbf{a}$ and $\mathbf{b}$ and filter lengths L_A and L_B, respectively. This results in the two-channel identification method depicted in **Figure 3**. The two-channel adaptive filter $\{A(q),\, B(q)\}$ minimizes

$$\frac{1}{N}\sum_{k=0}^{N-1} e_p^2[k], \tag{8}$$

with

$$e_p[k] = B(q)u[k] + A(q)y[k]. \tag{9}$$

To avoid the trivial solution $A(q) = B(q) = 0$, the first tap of $A(q)$ is set to 1: $\boxed{A(q) = 1 + q^{-1}\bar{A}(q)}$. We would like the filter $B(q)$ to identify the product $-H^{-1}(q)F(q)$ and the filter $A(q)$ to identify $H^{-1}(q)$ so that $e_p[k]$ equals $w[k]$. The feedback path estimate $\hat{F}(q)$ then corresponds to the IIR-filter $-A^{-1}(q)B(q)$. Hence, the filter $A^{-1}(q)$ should be constrained to be stable.

The inputs $u[k]$ and $y[k]$ of the two-channel adaptive filter are given as

$$u[k] = G(q)(y[k] - \hat{F}_0(q)u[k]) + r[k], \tag{10}$$

$$y[k] = F(q)u[k] + x[k], \tag{11}$$

where $r[k]$ is the probe signal (noise) injected at the loudspeaker input. Substituting (11) in (10) gives

$$u[k] = r[k] + C(q)x[k], \tag{12}$$

where $C(q)$ is the closed-loop system from $x[k]$ to $u[k]$

$$C(q) = \frac{G(q)}{1 - G(q)\left(F(q) - \hat{F}_0(q)\right)}. \tag{13}$$

Using (11)-(12), the output $e_p[k]$ of the two-channel adaptive filter equals

$$\begin{aligned} e_p[k] &= e_x[k] + e_r[k] && (14)\\ e_x[k] &= \left(A(q) + \frac{G(q)(B(q) + A(q)F(q))}{1 - G(q)(F(q) - \hat{F}_0(q))}\right) x[k] && (15)\\ e_r[k] &= \frac{B(q) + A(q)F(q)}{1 - G(q)(F(q) - \hat{F}_0(q))} r[k] && (16) \end{aligned}$$

Below, we study conditions under which minimization of (8), has the unique solution

$$A(q) = H^{-1}(q);\ B(q) = -H^{-1}(q)F(q) \tag{17}$$

so that $-A^{-1}(q)B(q)$ is an unbiased estimate of the feedback path $F(q)$. The conditions for identifiability also apply to the non-linear PEM criterion (6)-(7), provided that $H(q)$ is stable (so that $H^{-1}(q)$ does not have any zeros on the unit circle). To analyze (14)-(16), we distinguish between two cases: $r[k] = 0$ (no noise injection) and $r[k] \neq 0$ (noise injection). In the derivation of the identifiability conditions, we assume that $G(q) = q^{-d_1}\bar{G}(q)$ with $d_1 \geq 1$ and that $\bar{G}(q)$, $H^{-1}(q)$, $F(q)$ and $\hat{F}_0(q)$ are causal. In addition, we assume the sufficient order case for $A(q)$ and $B(q)$, i.e., $\boxed{L_A \geq L_{H^{-1}}}$ and $\boxed{L_B \geq L_{H^{-1}} + L_F - 1}$, so that $A(q)$ and $B(q)$ can model the desired solution (17). Section III-C considers the case of undermodelling.

A. *Case 1:* $r[k] = 0$ *(no noise injection)*

If $r[k] = 0$, minimization of $\frac{1}{N}\sum_{k=0}^{N-1} e_p^2[k]$ reduces to minimization of

$$\frac{1}{N}\sum_{k=0}^{N-1} e_x^2[k] \tag{18}$$

with $e_x[k]$ defined in (15).

Lemma 1: Assume that $x[k] = H(q)w[k]$ with $w[k]$ white noise and $H^{-1}(q) = 1 + q^{-1}P(q)$ an FIR filter. Then, minimization of (18) with $A(q) = 1 + q^{-1}\bar{A}(q)$ results in the unique desired solution (17) if at least one of the following conditions is satisfied:

- The forward path $G(q)$ has a delay $\boxed{d_1 \geq L_A}$;

- The cancellation path $B(q)$ has a delay d_2 with $\boxed{d_1+d_2 \geq L_A}$, i.e., $B(q)=q^{-d_2}\bar{B}(q)$ and the feedback path $F(q)$ has a delay of at least d_2 samples, i.e., $\boxed{F(q)=q^{-d_2}\bar{F}(q)}$.
- $\bar{G}(q)$ or $\hat{F}_0(q)$ are time-varying or $\bar{G}(q)$ is nonlinear.

Proof: Since $G(q)=q^{-d_1}\bar{G}(q)$ with $d_1 \geq 1$ and $\bar{G}(q)$, $F(q)$, $\hat{F}_0(q)$, $A(q)$, $B(q)$ are causal, $e_x[k]$ can be written as

$$e_x[k]=\Big(A(q)+q^{-d_1}\Gamma(q)\Big)\,x[k], \tag{19}$$

where

$$\Gamma(q)=\frac{\bar{G}(q)(B(q)+A(q)F(q))}{1-q^{-d_1}\bar{G}(q)(F(q)-\hat{F}_0(q))} \tag{20}$$

is a causal IIR filter, which may be specified as $\Gamma(q)=\gamma_0+q^{-1}\gamma_1+....$ Since $d_1 \geq 1$, the first tap of $A(q)+q^{-d_1}\Gamma(q)$ in (19) equals the first tap $a_0=1$ of $A(q)$ and hence, minimization of $\frac{1}{N}\sum_{k=0}^{N-1}e_x^2[k]=\frac{1}{N}\sum_{k=0}^{N-1}\left[\big(A(q)+q^{-d_1}\Gamma(q)\big)\,x[k]\right]^2$ corresponds to a linear prediction of $x[k]$.

If $x[k]=H(q)w[k]$ with $w[k]$ white noise, the optimal solution corresponds to

$$\boxed{A(q)+q^{-d_1}\Gamma(q)=A(q)+q^{-d_1}\frac{\bar{G}(q)(B(q)+A(q)F(q))}{1-q^{-d_1}\bar{G}(q)(F(q)-\hat{F}_0(q))}=H^{-1}(q)=1+q^{-1}P(q),} \tag{21}$$

or

$$1+a_1q^{-1}+\ldots+a_{d_1-1}q^{-d_1+1}+(a_{d_1}+\gamma_0)q^{-d_1}+\ldots=1+p_0q^{-1}+\ldots+p_{P-1}q^{-L_P}. \tag{22}$$

In general, $A(q)$ and $B(q)$ are not uniquely determined by equating coefficients of equal powers of q on both sides in (21) or (22). Below, we derive conditions under which the solution to (21) is unique and equals the desired solution (17).

- **Delay d_1 in the forward path $G(q)$**

  If the delay $d_1 \geq L_A \geq L_P+1=L_{H^{-1}}$, (22) has the unique solution

  $$A(q)=1+q^{-1}P(q)=H^{-1}(q) \quad \text{and} \quad \Gamma(q)=0. \tag{23}$$

  Since $a_0=1$, the equation $\Gamma(q)=0$ is satisfied if and only[3] if $B(q)=-A(q)F(q)$, resulting in the desired solution (17).

- **Delay d_2 in the cancellation path**

[3]Note that this assumes that $G(e^{j\omega}) \neq 0$ for all $\omega \in [0,\pi]$. At angular frequencies ω where $G(e^{j\omega})=0$, the feedback path cannot be identified. However, at those frequencies, no instability can occur and hence no feedback cancellation is required.

If the cancellation path $B(q)$ has a delay d_2, i.e., $B(q) = q^{-d_2}\bar{B}(q)$ and the feedback path $F(q)$ has a delay of at least d_2 samples, i.e., $F(q) = q^{-d_2}\bar{F}(q)$, (21) can be expressed as

$$A(q) + q^{-d_1-d_2}\bar{\Gamma}(q) = A(q) + q^{-d_1-d_2}\frac{\bar{G}(q)(\bar{B}(q) + A(q)\bar{F}(q))}{1 - q^{-d_1}\bar{G}(q)(F(q) - \hat{F}_0(q))} = H^{-1}(q). \qquad (24)$$

If $d_2 + d_1 \geq L_A \geq L_{H^{-1}}$, the solution of (24) is unique and equals

$$A(q) = H^{-1}(q); \qquad \bar{B}(q) = -A(q)\bar{F}(q). \qquad (25)$$

- **Time-varying $\hat{F}_0(q)$, $\bar{G}(q)$ or nonlinear $\bar{G}(q)$**

  In general, (21) implies that there are several solutions for $A(q)$ and $B(q)$. If $\bar{G}(q)$ or $\hat{F}_0(q)$ are time-varying, equation (21) (or (22)) and hence, the positions of the spurious solutions will change with time. Several different equations (21) then have to be satisfied, one for each time segment, so that it is likely that –with sufficient averaging– the algorithm will converge to the desired solution. Hence, if $\hat{F}_0(q)$ is at each time instant replaced by the most recent estimate of $-A^{-1}(q)B(q)$, the adaptive filters may converge to the desired solution, even without adding a delay in $G(q)$.

  A nonlinear $\bar{G}(q)$ reduces the correlation between $x[k]$ and $\frac{\bar{G}(q)}{(1-q^{-d_1}\bar{G}(q)(F(q)-\hat{F}_0(q)))}x[k]$ so that it decouples the minimization of $\frac{1}{N}\sum_{k=0}^{N-1} e_x^2[k]$ (cf. (15)) into a minimization of $\frac{1}{N}\sum_{k=0}^{N-1}\left(A(q)x[k]\right)^2$ and $\frac{1}{N}\sum_{k=0}^{N-1}\left[\left(B(q) + A(q)F(q)\right)x[k]\right]^2$. If $w[k]$ is white noise, both terms are minimized if and only if $A(q)$ and $B(q)$ equal the desired solution (17).

■

Lemma 1 shows that adding a delay d_1 to the forward path $G(q)$ and/or a delay d_2 to the cancellation path with $d = d_1 + d_2 \geq L_A$ renders the system $\{F(q),\, H^{-1}(q)\}$ identifiable. Adding a delay d_2 to the cancellation path only results in an unbiased feedback path estimate if the first d_2 taps of $F(q)$ equal 0. A delay in the feedback path may arise from the propagation time of the sound from the loudspeaker to the microphone and the processing delay of the DAC and ADC converters. Since most audio signals such as speech, can be modelled by an all-pole model $H(q)$, the filter $H^{-1}(q)$ is usually much shorter than $H(q)$. Hence, the minimum required delay $d = d_1 + d_2 = L_{H^{-1}}$ is smaller than the delay that is needed in the standard CAF to decorrelate $x[k]$ and $u[k]$. Note that the delay d_1 in the forward path $G(q)$ of the hearing aid should be kept small in order not to degrade intelligibility [26] and sound quality [20], [27].

Remark 1: The above derived identifiability conditions assume that the excitation $w[k]$ of the AR-model $H(q)$ is white noise. This assumption does not apply for periodic signals $x[k]$ such as a pure sinusoid or a voiced speech segment, where the frequency spectrum consists of discrete pulses. For periodic signals, the filter $A(q) + q^{-d_1}\Gamma(q)$ (see (21)) tries to cancel the discrete frequency pulses. As a result, the feedback path $F(q)$ cannot be identified if $r[k] = 0$.

To illustrate this, consider e.g., a voiced speech signal $x[k]$. The excitation $w[k]$ of voiced speech resembles a periodic impulse train with pitch period P, so that a voiced speech signal $x[k]$ can be reasonably approximated by a periodic signal with period P and hence, by a sum of harmonics [28]:

$$x[k] = \sum_{i=1}^{L_h} c_i \cos(2\pi i \frac{f_0}{f_s} k + \phi_i), \tag{26}$$

where c_i and ϕ_i denote the amplitude and phase of the i-th harmonic, $f_0 = \frac{1}{P}$ is the pitch frequency and L_h is the number of harmonics given by[4] $L_h = \left\lfloor \frac{f_s}{2f_0} \right\rfloor$ with $f_s = 16$ kHz the sampling frequency. For this periodic signal $x[k]$, the error $\frac{1}{N}\sum_{k=0}^{N-1} e_x^2[k]$ equals 0 if

$$A(q) + q^{-d_1}\Gamma(q) = Q(q)\Pi_{i=1}^{L}(1 - e^{j2\pi i \frac{f_0}{f_s}} q^{-1})(1 - e^{-j2\pi i \frac{f_0}{f_s}} q^{-1}), \tag{27}$$

where, $Q(q)$ is any random polynomial. Hence, the filter $A(q) + q^{-d_1}\Gamma(q)$ will not model $H^{-1}(q)$ but will try to cancel the impulse train by putting notches at the normalized frequencies $\frac{if_0}{f_s}$ with $i \in \mathbb{N}$ and $\frac{if_0}{f_s} \leq \frac{1}{2}$ [28]. Consequently, the feedback path $F(q)$ cannot be identified.

B. Case 2: $r[k] \neq 0$ (noise injection)

Lemma 2: Assume that $x[k] = H(q)w[k]$ where $w[k]$ is white noise. Then, minimization of (8) results in the unique desired solution (17) if $r[k] \neq 0$ and $r[k]$ and $x[k]$ are uncorrelated.

Proof: If $r[k] \neq 0$ and $r[k]$ and $x[k]$ are uncorrelated, the cost function $\frac{1}{N}\sum_{k=0}^{N-1} e_p^2[k]$ equals

$$\frac{1}{N}\sum_{k=0}^{N-1} e_x^2[k] + \frac{1}{N}\sum_{k=0}^{N-1} e_r^2[k], \tag{28}$$

with $e_x[k]$ and $e_r[k]$ defined in (15)-(16). If there exist an $A(q)$ and $B(q)$ that minimize both $\frac{1}{N}\sum_{k=0}^{N-1} e_x^2[k]$ and $\frac{1}{N}\sum_{k=0}^{N-1} e_r^2[k]$ (which is the case if $L_B \geq L_{H^{-1}} + L_F - 1$ and $L_A \geq L_{H^{-1}}$), then these $A(q)$ and $B(q)$ are the solution to the minimization of (28). The term $\frac{1}{N}\sum_{k=0}^{N-1} e_r^2[k]$ is minimized if

$$\boxed{B(q) + A(q)F(q) = 0,} \tag{29}$$

which results in a true estimate $-A^{-1}(q)B(q)$ of the feedback path $F(q)$ provided that $A^{-1}(q)$ is stable. If $w[k]$ is white noise and $G(q)$ contains a delay $d_1 \geq 1$, $\frac{1}{N}\sum_{k=0}^{N-1} e_x^2[k]$ is minimized if (21) is satisfied (cf. the proof of Lemma 1). Both (21) and (29) are fulfilled if and only if $A(q) = H^{-1}(q)$ and $B(q) = H^{-1}(q)F(q)$. Hence, the optimal solution is found to be unique and to equal the desired solution. ■

Note that if the level of the noise signal $r[k]$ is too low compared to the level of $x[k]$, the error energy $\frac{1}{N}\sum_{k=0}^{N-1} e_r^2[k]$ is negligible compared to $\frac{1}{N}\sum_{k=0}^{N-1} e_x^2[k]$. If the identifiability conditions derived

[4] *$\lfloor x \rfloor$ returns the largest integer smaller than or equal to x.*

in Section III-A are not satisfied, several solutions $A(q)$ and $B(q)$ exist if $r[k] = 0$ so that, for $r[k] \rightarrow 0$, the identification problem may become ill-conditioned. The level of $r[k]$ thus determines the condition of the identification problem and hence the convergence.

C. Biased feedback path estimate in case of undermodelling

Section III-A shows that adding a delay in the forward path $G(q)$ and/or in the cancellation path can render the system identifiable without adding a probe signal $r[k]$ or non-linearities. If the total delay $d = d_1 + d_2$ with d_1 the delay in $G(q)$ and d_2 the common delay in the feedback $F(q)$ and the cancellation path $B(q)$, exceeds L_A an unbiased estimate $A^{-1}(q)B(q)$ is obtained. The derivation of the identifiability conditions assumes the sufficient order case for $A(q)$ and $B(q)$, i.e., $L_A \geq L_{H^{-1}}$ and $L_B \geq L_{H^{-1}} + L_F - 1$. In practice, the filter length L_{H-1} of the inverse speech model $H^{-1}(q)$ and the filter length L_F of the feedback path $F(q)$ are unknown, so that undermodelling may occur, i.e., $L_A < L_{H^{-1}}$ or/and $L_B < L_A + L_F - 1$. In this case, the solution to (21) is still unique if $d \geq L_A$ but biased. In this section, we show that –like for the standard CAF [10] or the filtered-X algorithm with fixed noise model $\hat{H}(q)$ [21]– the amount of bias depends on the amplitude characteristic of the closed-loop system, the delay d and –for $r[k] \neq 0$ with $r[k]$ and $x[k]$ uncorrelated– the power spectral density of the probe signal $r[k]$.

- The larger the amplitude characteristic of the closed-loop system $C(q)$ (see (13)) at angular frequency ω, the smaller the bias of the feedback path estimate at this angular frequency ω. Hence, the bias of the feedback path estimate will be smallest at the critical frequencies, which is a desired property.

  Proof: Consider minimization of (18). The term $(B(q)+A(q)F(q))$ in $e_x[k]$ is weighted by the closed-loop system $C(q)$ (see (15)). Hence, the larger $\left|C(e^{j\omega})\right|$, the smaller the bias in the feedback path estimate $\hat{F}(q) = -A^{-1}(q)B(q)$ at angular frequency ω. ■

- Increasing the delay d for a given L_A will in general reduce the bias if $w[k]$ is white.

  Proof: If $w[k]$ is white noise, $q^{-d}w[k]$ is uncorrelated with $q^{-l}w[k]$ for $l = 0, \cdots, d-1$, so that minimization of $\frac{1}{N}\sum_{k=0}^{N-1} e_x^2[k]$ corresponds to a minimization of $\frac{1}{N}\sum_{k=0}^{N-1} e_a^2[k] + \frac{1}{N}\sum_{k=0}^{N-1} e_b^2[k]$, with

$$e_a[k] = [A(q)H(q)]_{1:d}\, w[k], \tag{30}$$

$$e_b[k] = [A(q)H(q)]_{d+1:end}\, w[k] + \frac{G(q)(B(q)+A(q)F(q))}{1 - G(q)(F(q) - \hat{F}_0(q))} H(q)w[k], \tag{31}$$

  where $[A(q)H(q)]_{1:d}$ is the filter whose impulse response corresponds to the first d coefficients of $A(q)H(q)$ and has zeros everywhere else and $[A(q)H(q)]_{d+1:end}$ is the filter that has zeros in the

first d positions, but otherwise is the same as the impulse response $A(q)H(q)$. The adaptive filter $B(q)$ attempts to minimize $\frac{1}{N}\sum_{k=0}^{N-1} e_b^2[k]$: if $[A(q)H(q)]_{d+1:end} \neq 0$, the feedback path estimate $\hat{F}(q) = -A^{-1}(q)B(q)$ is biased. Since in most cases the impulse response of $H(q)$ and hence, $A(q)H(q)$ decreases with increasing lag, increasing the delay d for a given fixed L_A will generally reduce the term $[A(q)H(q)]_{d+1:end}\, w[k]$ and hence, the bias of the estimate $\hat{F}(q)$ [21]. ■

- Inserting a probe signal $r[k]$ with $r[k]$ and $x[k]$ uncorrelated, reduces the bias of the feedback path estimate: the larger the power spectral density $\left|R(e^{j\omega})\right|^2$ with $R(e^{j\omega})$ the spectrum of $r[k]$, the smaller the bias at angular frequency ω.

  Proof: Increasing $\left|R(e^{j\omega})\right|^2$ puts more weight on the error term $\frac{1}{N}\sum_{k=0}^{N-1} e_r^2[k]$ at angular frequency ω and hence, reduces the bias of $\hat{F}(q) = -A^{-1}(q)B(q)$ at angular frequency ω. ■

IV. RECURSIVE IDENTIFICATION

Section III shows that under certain conditions the feedback path $F(q)$ and the inverse signal model $H^{-1}(q)$ are both identifiable even if no additional noise $r[k]$ is injected in the system and no non-linearities are inserted in $G(q)$. In this section, two different recursive procedures for estimating the feedback path $F(q)$ and the desired signal model $H(q)$ are proposed based on the two-channel identification method of Section III and the PEM of Section II, resulting in a two-channel adaptive feedback canceller (2-ch AFC) and an PEM based adaptive feedback canceller (PEM-AFC).

The *two-channel identification method* of Figure 3 has the advantage of having a linear cost function. However, to obtain the feedback path estimate $\hat{F}(q)$, the adaptive filter $-B(q)$ has to be multiplied by $A^{-1}(q)$. Hence, a stability constraint should be imposed on $A^{-1}(q)$. The *prediction error method* estimates $F(q)$ and $H^{-1}(q)$ instead of $-H^{-1}(q)F(q)$ and $H^{-1}(q)$, but has a non-linear optimization criterion. Filtering with $A^{-1}(q)$ is then not required and shorter adaptive filters can be used. In practice, the desired signal $x[k]$ is often highly time-varying, while the feedback path varies more slowly in time. In contrast to the 2-ch AFC, the PEM-AFC allows to use a different adaptation scheme or adaptation speed for estimating the feedback path $F(q)$ and the inverse desired signal model $H^{-1}(q)$ and hence, is found to be preferable for highly non-stationary desired signals.

A. Two-channel adaptive feedback canceller (2-ch AFC)

At each time instant k, the two-channel adaptive filter $\begin{bmatrix} \mathbf{a}^T & \mathbf{b}^T \end{bmatrix}^T$ in Figure 3 minimizes

$$J_k(\mathbf{a},\mathbf{b}) = \sum_{\bar{k}=1}^{k} \lambda^{k-\bar{k}} e_p^2[\bar{k}], \tag{32}$$

with $e_p[\bar{k}] = B(q)u[\bar{k}] + A(q)y[\bar{k}]$ (see (9)). A forgetting factor $\lambda \in (0, 1]$ has been inserted in (32) to allow for tracking in time-varying scenarios. To avoid the trivial solution $\mathbf{a} = \mathbf{0}$, $\mathbf{b} = \mathbf{0}$, the first coefficient of $\mathbf{a}$ is set to one, resulting in

$$e_p[\bar{k}] = y[\bar{k}] + \mathbf{b}^T\mathbf{u}[\bar{k}] + \bar{\mathbf{a}}^T\bar{\mathbf{y}}[\bar{k}], \tag{33}$$

with

$$\bar{\mathbf{a}}^T = \left[\begin{array}{cccc} a_1 & a_2 & \cdots & a_{L_A-1} \end{array} \right], \tag{34}$$

$$\mathbf{u}[\bar{k}] = \left[\begin{array}{cccc} u[\bar{k}] & u[\bar{k}-1] & \cdots & u[\bar{k}-L_B+1] \end{array} \right]^T \tag{35}$$

$$\bar{\mathbf{y}}[\bar{k}] = \left[\begin{array}{cccc} y[\bar{k}-1] & y[\bar{k}-2] & \cdots & y[\bar{k}-L_A+1] \end{array} \right]^T \tag{36}$$

The cost function (32) is *linear* in the filters $\bar{\mathbf{a}}$ and $\mathbf{b}$ so that standard recursive algorithms such as modified LMS [29] and RLS [30] can be used. In the sequel, RLS will be used to update $\bar{\mathbf{a}}$ and $\mathbf{b}$:

$$\left[\begin{array}{c} \bar{\mathbf{a}}[k] \\ \mathbf{b}[k] \end{array} \right] = \left[\begin{array}{c} \bar{\mathbf{a}}[k-1] \\ \mathbf{b}[k-1] \end{array} \right] - \mathbf{R^{-1}}[k] \left[\begin{array}{c} \bar{\mathbf{y}}[k] \\ \mathbf{u}[k] \end{array} \right] \epsilon_p[k], \tag{37}$$

$$\mathbf{R}[k] = \lambda\mathbf{R}[k-1] + \left[\begin{array}{c} \bar{\mathbf{y}}[k] \\ \mathbf{u}[k] \end{array} \right] \left[\begin{array}{cc} \bar{\mathbf{y}}^T[k] & \mathbf{u}^T[k] \end{array} \right], \tag{38}$$

with $\epsilon_p[k]$ the a priori residual, defined as

$$\epsilon_p[k] = y[k] + \mathbf{b}^T[k-1]\mathbf{u}[k] + \bar{\mathbf{a}}^T[k-1]\bar{\mathbf{y}}[k]. \tag{39}$$

Below, we consider two different scenarios for the 2-ch AFC, i.e., the case where the feedback canceller $\hat{F}_0(q)$ is kept fixed during adaptation and the case where $\hat{F}_0(q)$ is updated during adaptation.

1) Feedback canceller $\hat{F}_0(q)$ is kept fixed during adaptation: If the filter $\hat{F}_0(q)$ in the feedback cancellation path is kept fixed during adaptation and the closed-loop system $C(q)$ (see (41)) is stable, the input data $u[k]$ and $y[k]$ are bounded so that convergence of the adaptive filters $\bar{\mathbf{a}}$ and $\mathbf{b}$ is guaranteed provided that $\mathbf{R}[k]$ is non-singular.

The feedback path estimate $\hat{F}(q)$ corresponds to the IIR-filter $-A^{-1}(q)B(q)$. To guarantee a stable feedback path estimate, a stability constraint on $A^{-1}(q)$ is thus required. The adaptive filters should therefore only be updated when the update results in a stable filter $A^{-1}(q)$. A simple (conservative) test for stability is to check that $\sum_{i=1}^{L_A-1} |a_i|$ is less than 1 [31]. All unstable updates will be detected by this approach, but the test may indicate that $A^{-1}(q)$ is unstable when it is not. For a stable model $H^{-1}(q) = 1 + q^{-1}P(q)$ with $\sum_{i=0}^{L_P-1} |p_i| \geq 1$, convergence of $A(q)$ to the optimal solution $H^{-1}(q)$ may then never be reached. A better, but computationally more complex approach, is to test after each update that the zeros of $A(q)$ lie inside the unit circle by using the Shur-Cohn test [31].

2) Feedback canceller $\hat{F}_0(q)$ is updated during adaptation: In practice, the feedback canceller $\hat{F}_0(q)$ is replaced during adaptation with new estimates $\hat{F}(q) = -A^{-1}(q)B(q)$ of the feedback path $F(q)$. Typically, $\hat{F}_0(q)$ is updated at the adaptation rate of the filters $A(q)$ and $B(q)$ (i.e., after each time instant k), but it may also be updated at a lower rate, e.g., after each T time instants. The input-output data $u[k]$, $y[k]$ used for identification are then determined by the adaptive filters $\mathbf{a}[\bar{k}]$ and $\mathbf{b}[\bar{k}]$ with $\bar{k} \leq k-1$. E.g., if $\hat{F}_0(q)$ is updated at the adaptation rate of $A(q)$ and $B(q)$, $u[k]$ can be efficiently computed as:

$$u[k] \quad = \quad r[k] + G(q)A^{-1}(q, k-1)\epsilon_p[k] \tag{40}$$

with $\epsilon_p[k]$ the a priori residual defined in (39). To guarantee convergence of the adaptive filters $\mathbf{a}$ and $\mathbf{b}$, a boundness condition must now be satisfied, namely, $u[k]$ and $y[k]$ should be bounded. Therefore, the filters $\mathbf{a}[\bar{k}]$ and $\mathbf{b}[\bar{k}]$ (with $\bar{k} = n \cdot T$ ($n \in \mathbb{N}$) and $\bar{k} \leq k-1$) should not result in an unstable closed-loop system $C(q, \bar{k})$

$$C(q, \bar{k}) = \frac{G(q)}{1 - G(q)\left(F(q) - A^{-1}(q, \bar{k})B(q, \bar{k})\right)} \tag{41}$$

for a significant length of time [32].

From simulations, we observed that, when $\hat{F}_0(q)$ is continuously being updated by $\hat{F}(q)$, the 2-ch AFC has a self-stabilizing feature whereby unstable poles of the closed-loop system $C(q)$ have a tendency to migrate back into the stable region. Since a stable $C(q)$ implies a stable feedback path estimate $\hat{F}(q, k-1) = -A^{-1}(q, k-1)B(q, k-1)$, a stability constraint on $A(q)$ is then not required. This is illustrated in Remark 5 of Section V-B. The self-stabilizing feature can be understood intuitively: if, for example, the feedback path estimate $\hat{F}(q, k-1)$ at time instant $k-1$ results in a closed-loop system $C(q, k-1)$ that is close to instability, the error $B(q) + A(q)F(q)$ in the feedback path estimate gets a large weight $C(q, k-1)$ in the prediction error $e_x[k]$ (see (15) and Section III-C), so that the next estimate $\hat{F}(q, k) = -A(q, k)^{-1}B(q, k)$ will get close to $F(q)$ and thus stabilizes the closed-loop system again. As a result, $u[k]$ and $y[k]$ remain bounded and $A(q, k)$ and $B(q, k)$ are found to converge to the desired solution if the identifiability conditions are satisfied. Due to the self-stabilizing property, faster convergence may be obtained than when $\hat{F}_0(q)$ is kept fixed. E.g., if the correlation matrix $\mathbf{R}[k]$ is initialized with a small identity matrix, the initial updates of the 2-ch AFC may be quite large. Because of the presence of the near-end signal $x[k]$, these initial updates are quite noisy so that the closed-loop system may become unstable. Simulations indicated that, if this occurs, $\hat{F}(q)$ sometimes immediately converges to the true feedback path $F(q)$.

B. PEM based adaptive feedback canceller (PEM-AFC)

The 2-ch AFC of Section IV-A estimates the product $F(q)H^{-1}(q)$ and the inverse signal model $H^{-1}(q)$. Hence, a joint adaptation algorithm and/or adaptation speed is required for $F(q)$ and $H^{-1}(q)$. In practice, the desired signal $x[k]$ is, e.g., a speech signal and thus strongly time-varying: the inverse speech model $H^{-1}(q)$ is only stationary during approximately 20 ms. To obtain a good estimate of the instantaneous speech model, fast convergence is required for the filter $A(q)$. However, the identification of the feedback path is strongly degraded by the presence of the desired signal $x[k]$ because of its high-energy with respect to the feedback signal $F(q)u[k]$. As a consequence, a large amount of data samples N (or a slow convergence time) is required to produce a reliable feedback path estimate (i.e., N corresponds to a duration $\gg 20$ ms), especially for small $|G(q)F(q)|$. Therefore, it seems preferable to use a different adaptation speed for the estimation of the slowly time-varying feedback path $F(q)$ on the one hand and the estimation of the highly time-varying inverse speech model $H^{-1}(q)$ on the other hand. Instead of estimating the product $F(q)H^{-1}(q)$ and $H^{-1}(q)$, the PEM directly estimates $F(q)$ and $H^{-1}(q)$. By introducing some approximations in the Hessian, the joint prediction error update equation for estimating $F(q)$ and $H^{-1}(q)$ decouples into two separate update equations for the two models, making a different adaptation possible. Below, we first describe the full PEM based adaptive feedback canceller and then consider the PEM based feedback canceller with a decoupled adaptation.

1) Full PEM based adaptive feedback canceller (PEM-AFC): **Figure 4** illustrates the PEM-AFC: the filter $A(q)$ estimates $H^{-1}(q)$ and the filter $\hat{F}(q)$ estimates $F(q)$. At each time instant k, the PEM minimizes

$$J_k(\bar{\mathbf{a}}, \hat{\mathbf{f}}) = \sum_{\bar{k}=1}^{k} \lambda^{k-i} e_p^2[\bar{k}], \tag{42}$$

where, $\lambda \in (0, 1]$ is the forgetting factor, $\mathbf{a}$ and $\hat{\mathbf{f}}$ are the coefficient vectors of $A(q)$ and $\hat{F}(q)$, defined as

$$\mathbf{a} = \begin{bmatrix} 1 & \bar{\mathbf{a}} \end{bmatrix}^T ; \hat{\mathbf{f}} = \begin{bmatrix} \hat{f}_0 & \hat{f}_1 & \cdots & \hat{f}_{L_{\hat{F}}-1} \end{bmatrix}^T, \tag{43}$$

and $e_p[\bar{k}]$ is the prediction error at time instant $\bar{k}$ given by

$$e_p[\bar{k}] = A(q)\left(y[\bar{k}] - \hat{F}(q)u[\bar{k}]\right). \tag{44}$$

The cost function $J_k(\bar{\mathbf{a}}, \hat{\mathbf{f}})$ is *non-linear* in the parameters $\bar{\mathbf{a}}$ and $\hat{\mathbf{f}}$. Hence, local minima exist and convergence to the global minimum is not guaranteed. In the sequel, we use the stochastic Gauss-Newton

update equation [32], i.e.,

$$\begin{bmatrix} \bar{\mathbf{a}}[k] \\ \hat{\mathbf{f}}[k] \end{bmatrix} = \begin{bmatrix} \bar{\mathbf{a}}[k-1] \\ \hat{\mathbf{f}}[k-1] \end{bmatrix} - \mathbf{R}[k]^{-1}\frac{1}{2}\mathbf{J}_k^{'}(\bar{\mathbf{a}}[k-1], \hat{\mathbf{f}}[k-1]), \tag{45}$$

where, $\mathbf{J}_k^{'}$ is the gradient of J_k computed using $\bar{\mathbf{a}}[k-1]$ and $\hat{\mathbf{f}}[k-1]$ as

$$\mathbf{J}_k^{'} = 2\begin{bmatrix} \frac{\partial \epsilon_p[k]}{\partial \bar{\mathbf{a}}[k-1]} \\ \frac{\partial \epsilon_p[k]}{\partial \hat{\mathbf{f}}[k-1]} \end{bmatrix} \epsilon_p[k], \tag{46}$$

$$\epsilon_p[k] = A(q,k-1)\Big(y[k] - \hat{F}(q,k-1)u[k]\Big) \tag{47}$$

and where

$$\mathbf{R}[k] = \lambda\mathbf{R}[k-1] + \begin{bmatrix} \frac{\partial \epsilon_p[k]}{\partial \bar{\mathbf{a}}[k-1]} \\ \frac{\partial \epsilon_p[k]}{\partial \hat{\mathbf{f}}[k-1]} \end{bmatrix} \begin{bmatrix} \left(\frac{\partial \epsilon_p[k]}{\partial \bar{\mathbf{a}}[k-1]}\right)^T & \left(\frac{\partial \epsilon_p[k]}{\partial \hat{\mathbf{f}}[k-1]}\right)^T \end{bmatrix}. \tag{48}$$

As in [32, chapter 2], the a priori prediction error $\epsilon_p[k]$ and the derivatives $\frac{\partial \epsilon_p[k]}{\partial \bar{\mathbf{a}}[k-1]}$ and $\frac{\partial \epsilon_p[k]}{\partial \hat{\mathbf{f}}[k-1]}$ are, for reasons of efficiency[5], approximated as:

$$\epsilon_p[k] = A(q,k-1)\epsilon[k], \tag{49}$$

$$\frac{\partial \epsilon_p[k]}{\partial \bar{\mathbf{a}}[k-1]} = \begin{bmatrix} \epsilon[k-1] & \epsilon[k-2] & \cdots & \epsilon[k-L_A+1] \end{bmatrix}^T, \tag{50}$$

$$\frac{\partial \epsilon_p[k]}{\partial \hat{\mathbf{f}}[k-1]} = -\begin{bmatrix} u_p[k] & u_p[k-1] & \cdots & u_p[k-L_{\hat{F}}+1] \end{bmatrix}^T, \tag{51}$$

where $\epsilon[k]$ and $u_p[k]$ are computed as:

$$\epsilon[k] = y[k] - \hat{F}(q,k-1)u[k] \tag{52}$$

$$u_p[k] = A(q,k-1)u[k]. \tag{53}$$

Note that this approximation assumes that $A(q,k-1) = A(q,k-\bar{k}_1)$ for $1 < \bar{k}_1 < L_{\hat{F}}$ and $\hat{F}(q,k-1) = \hat{F}(q,k-\bar{k}_2)$ for $1 < \bar{k}_2 < L_A$. Since L_A is rather small (e.g., 20 taps), it is reasonable to expect that $\hat{F}(q,k-1) = \hat{F}(q,k-\bar{k}_2)$ for $1 < \bar{k}_2 < L_A$. Furthermore in hearing aids, the dominant part of the true feedback path $F(q)$ is quite short, so that a relatively short filter length $L_{\hat{F}}$ is typically used for $\hat{F}(q)$ [3], i.e., $L_{\hat{F}}/f_s < 20$ ms (i.e., smaller than the short-time stationarity of speech). Hence, we expect that $A(q,k-1) = A(q,k-\bar{k}_1)$ for $1 < \bar{k}_1 < L_{\hat{F}}$, even for highly time-varying speech signals $x[k]$.

Remark 2: Again, a boundness condition must be satisfied if $\hat{F}_0(q)$ is updated during adaptation to guarantee convergence.

[5]Otherwise, $L_{\hat{F}} + L_A - 2$ additional filtering operations would be required, i.e., $A(q,k-1)u[k-i]$, $i = 1, \cdots, L_{\hat{F}} - 1$ and $\hat{F}(q,k-1)u[k-i]$, $i = 1, \cdots, L_A - 1$.

2) Decoupling the adaptation of $\hat{F}(q)$ and $A(q)$: The stochastic Gauss-Newton update equation (45) corresponds to a joint update equation for $\hat{\mathbf{f}}[k]$ and $\bar{\mathbf{a}}[k]$. Forcing the off-diagonal blocks of $\mathbf{R}[k]$ to zero decouples the update equations for the feedback path $\hat{\mathbf{f}}[k]$ and the noise model $\bar{\mathbf{a}}[k]$:

$$\begin{cases} \bar{\mathbf{a}}[k] = \bar{\mathbf{a}}[k-1] - \mathbf{R}_{\bar{\mathbf{a}}}^{-1}[k] \frac{\partial \epsilon_p[k]}{\partial \bar{\mathbf{a}}[k-1]} \epsilon_p[k] \\ \hat{\mathbf{f}}[k] = \hat{\mathbf{f}}[k-1] - \mathbf{R}_{\hat{\mathbf{f}}}^{-1}[k] \frac{\partial \epsilon_p[k]}{\partial \hat{\mathbf{f}}[k-1]} \epsilon_p[k] \end{cases} \tag{54}$$

with

$$\begin{cases} \mathbf{R}_{\bar{\mathbf{a}}}[k] = \lambda_{\bar{\mathbf{a}}}[k] \mathbf{R}_{\bar{\mathbf{a}}}[k-1] + \frac{\partial \epsilon_p[k]}{\partial \bar{\mathbf{a}}[k-1]} \left(\frac{\partial \epsilon_p[k]}{\partial \bar{\mathbf{a}}[k-1]} \right)^T \\ \mathbf{R}_{\hat{\mathbf{f}}}[k] = \lambda_{\hat{\mathbf{f}}}[k] \mathbf{R}_{\hat{\mathbf{f}}}[k-1] + \frac{\partial \epsilon_p[k]}{\partial \hat{\mathbf{f}}[k-1]} \left(\frac{\partial \epsilon_p[k]}{\partial \hat{\mathbf{f}}[k-1]} \right)^T. \end{cases} \tag{55}$$

Since the block-diagonal approximation

$$\begin{bmatrix} \mathbf{R}_{\bar{\mathbf{a}}}[k] & \mathbf{0} \\ \mathbf{0} & \mathbf{R}_{\hat{\mathbf{f}}}[k] \end{bmatrix} \tag{56}$$

of $\mathbf{R}[k]$ is positive semi-definite, (54) converges to a minimum (local or global) of $\mathbf{J}_k$, provided that the update equations (54) are stable[6] [32]. Algorithm (54)-(55) is expected to have a convergence rate in-between the convergence rate of the stochastic gradient algorithm (i.e., using $\mathbf{R}[k] = \frac{1}{\mu}\mathbf{I}$ with $\mathbf{I}$ the identity matrix) and the stochastic Gauss-Newton algorithm (45)-(48).

Different forgetting factors $\lambda_{\bar{\mathbf{a}}}[k]$ and $\lambda_{\hat{\mathbf{f}}}[k]$ or different adaptation schemes (e.g., stochastic Gauss-Newton or stochastic gradient adaptation) can now be used for $\bar{\mathbf{a}}$ and $\hat{\mathbf{f}}$. Because speech is short-term stationary for about $10-20$ ms, $\lambda_{\bar{\mathbf{a}}} = 1 - \frac{1}{160}$ seems a good choice for a sampling frequency $f_s = 16$ kHz.

The PEM-AFC does not require a filtering with $A^{-1}(q)$ so that a stability constraint on $A^{-1}(q)$ is not required. However, since the desired signal $x[k]$ is bounded, the model $H(q)$ is assumed to be stable or marginally stable. Hence, the performance of the non-linear PEM-AFC can be improved by limiting the search space for $A(q)$ to the inversely stable or marginally stable filters. This stability constraint can be easily imposed by using e.g., the Burg lattice algorithm [33] instead of RLS for updating the AR-coefficients $\bar{\mathbf{a}}$. The Burg lattice algorithm, described by **algorithm 1**, guarantees stability by ensuring that the reflection coefficients $\kappa_i \leq 1$, $i = 1, \cdots, L_A - 1$. The prediction error $\epsilon_p[k]$ and the derivative $\frac{\partial \epsilon_p[k]}{\partial \hat{\mathbf{f}}[k-1]}$ (see (49)-(53)) in (54) are then obtained by filtering the feedback compensated signal $\epsilon[k]$ and the loudspeaker signal $u[k]$, respectively, through the lattice filter determined by the reflection coefficients $\kappa_i[k-1]$ from the previous iteration. In the simulations, we concentrate on this particular implementation of the PEM-AFC, referred to as decoupled (lattice) PEM-AFC.

[6]In the simulations, no instability occurred. If needed, instability can be avoided by including a small step size $\mu < 1$ in the update equations (54).

Remark 3: If the stochastic gradient method is used to update the feedback canceller $\hat{F}(q)$, the decoupled (lattice) PEM-AFC corresponds to the feedback canceller proposed by [19]. In [19], the input $u[k]$ and the error $e[k]$ are also pre-whitened through adaptive lattice filters before updating the feedback canceller $\hat{F}(q)$. Originally, the idea of adaptive pre-whitening was proposed in [34] to improve the convergence rate of an LMS-based echo canceller. The algorithm in [19] has been derived from [34] by performing the adaptation of the lattice decorrelation filter on the feedback compensated signal $e[k]$ instead of on the input signal $u[k]$ to the feedback canceller. The LMS-based feedback canceller of [19] can thus also be interpreted as an implementation of the (decoupled) PEM-AFC so that the identifiability conditions derived in Section III also apply to [19]. In [19], however, no identifiability conditions have been derived.

Remark 4: Note that the update equation for the feedback path $\hat{\mathbf{f}}[k]$ corresponds to the filtered-X algorithm of [20]. If there is a group delay associated with the filter $A(q)$, changes to the adaptive filter $\hat{\mathbf{f}}[k]$ do not have an immediate impact on the error $\epsilon_p[k]$ of the filtered-X algorithm. As a consequence, the filtered-X algorithm may become unstable if the filter coefficients $\hat{\mathbf{f}}[k]$ change too quickly in time [17], [35]. In [36],[37] we show that a delayed adaptation can be avoided by computing the a priori prediction error $\epsilon_p[k]$ from the pre-filtered data $u_p[k]$ and $y_p[k] = A(q, k-1)u[k]$ instead of computing $\epsilon_p[k]$ by filtering the feedback-compensated signal $\epsilon[k]$ with $A(q, k-1)$ (cf. (49)).

V. Simulation results

In this section, we compare the performance of the 2-ch AFC and the decoupled PEM-AFC with the standard CAF algorithm[7] [6], [10] and the filtered-X algorithm with fixed $A(q)$ [20], [21] for both stationary and time-varying signals. All feedback cancellers are implemented using RLS with $\lambda = 1$. In the PEM-AFC, the filter $A(q)$ is implemented by the Burg lattice algorithm with $\lambda_{\bar{\mathbf{a}}} = 1 - \frac{1}{160}$. In the simulations, the filter $\hat{F}_0(q)$ in feedback cancellation path is continuously updated during adaptation with the estimate $\hat{F}(q)$. Among the different conditions for identifiability of $H(q)$ and $F(q)$, inserting a delay d_1 in the forward path seems the preferred option. Inserting a delay d_2 in the cancellation path only results in an unbiased feedback path estimate $\hat{F}(q)$ if the first d_2 taps of $F(q)$ are zero and adding non-linearities to $G(q)$ or inserting a noise signal $r[k]$ may degrade the sound quality. In the simulations we, therefore, concentrate on the influence of the delay d_1 in the forward path on the performance of the different algorithms. In the derivation of the identifiability conditions, we assumed that the desired signal

[7] i.e., the 2-ch AFC with fixed $A(q) = 1$.

$x[k]$ is generated by passing white noise $w[k]$ through an all-pole filter. If $x[k]$ is a speech signal, the excitation of voiced segments however corresponds to an impulse train, so that the performance of the feedback path cancellation techniques may be degraded. The importance of the white-noise assumption for the performance of the different techniques is evaluated.

In the simulations, the acoustic feedback path model $F(q)$ is an FIR filter with filter length $L_F = 50$, obtained from a measured feedback path. The frequency characteristic of $F(q)$ is depicted in **Figure 5**. The forward path $G(q)$ equals $q^{-d_1}|G|$ with $|G| = 5$. The sampling frequency $f_s = 16$ kHz. Without feedback cancellation, the maximum stable gain (cf. Section V-A) equals 14.63 dB. Unless specified otherwise, the filter lengths L_A, L_B and $L_{\hat{F}}$ of the adaptive filters $A(q)$ in the 2-ch AFC and PEM-AFC, $B(q)$ in the 2-ch AFC and $\hat{F}(q)$ in the CAF, the PEM-AFC and the filtered-X algorithm are set to $L_A = 21$, $L_B = L_A + L_F - 1$ and $L_{\hat{F}} = L_F = 50$.

A. Performance measures

To assess the performance of feedback cancellation algorithms we use the misalignment $\zeta(F(q), \hat{F}(q))$ between the true and estimated feedback path $\hat{F}(q)$ and the maximum and added stable gain [3].

The *misalignment* $\zeta(F(q), \hat{F}(q))$ is computed in the frequency domain as

$$\zeta(F(q), \hat{F}(q)) = \frac{\sum_{k=0}^{N_f-1} \left| F(e^{j\pi\frac{k}{N_f}}) - \hat{F}(e^{j\pi\frac{k}{N_f}}) \right|^2}{\sum_{k=0}^{N_f-1} \left| F(e^{j\pi\frac{k}{N_f}}) \right|^2}, \tag{57}$$

where $N_f = 512$ equals the number of frequency points.

In [3], the *maximum stable gain* MSG is defined as the maximum allowable gain assuming a flat frequency response $G(q)$ for the hearing aid:

$$\text{MSG} = 20\log_{10}\left(\min_{\omega} \frac{1}{|F(e^{j\omega}) - \hat{F}(e^{j\omega})|}\right). \tag{58}$$

The MSG is determined by the frequency where the mismatch between the true feedback path $F(q)$ and the feedback path estimate $\hat{F}(q)$ is the largest. The system will however only be unstable when the phase at that frequency equals $2\pi n$ [5]. The *added stable gain* ASG is defined as the additional gain that is possible by using the feedback canceller $\hat{F}(q)$, i.e.,

$$\text{ASG=MSG-}20\log_{10}\left(\min_{\omega} \frac{1}{|F(e^{j\omega})|}\right). \tag{59}$$

B. Simulation results: stationary desired signal $x[k]$

In this section, the performance of the 2-ch AFC and the decoupled PEM-AFC are evaluated for a stationary *speech-shaped noise signal* $x[k]$ created by passing Gaussian noise through a 20-th order all-pole filter $H(q)$. The impulse response of $H(q)$ is depicted in **Figure 6**.

Figure 7 plots the misalignment $\zeta(F,\hat{F})$ and the ASG of the CAF, the 2-ch AFC and the PEM-AFC as a function of the delay d_1 in the forward path. For comparison, the misalignment $\zeta(F,\hat{F})$ of the feedback path estimate obtained with filtered-X RLS using the correct speech model, i.e., $A(q)=H^{-1}(q)$, which we consider in some sense an optimal solution, is depicted too. The filter lengths of the adaptive filters are set to the true model orders, i.e. $L_A=L_{H^{-1}}=21$, $L_B=L_{H^{-1}}+L_F-1$ in the 2-ch AFC and $L_{\hat{F}}=L_F$ in the CAF, the PEM-AFC and the optimal filtered-X algorithm. Figure 7 illustrates the condition for identifiability: if the delay $d_1 \geq L_A$, the 2-ch AFC and the PEM-AFC obtain an unbiased feedback path estimate. The 2-ch AFC and PEM-AFC perform nearly as well as the optimal filtered-X algorithm and clearly outperform the CAF. If $d_1 < L_A$, the feedback path $F(q)$ and the model $H^{-1}(q)$ are not both identifiable: multiple spurious solutions for the feedback path $F(q)$ then exist. If $d_1 < L_A$, the correlation matrix $\mathbf{R}[k]$ in (38) that is used in the update equation of the 2-ch AFC is singular and hence, instability occurs. The performance of the CAF improves with increasing delay d_1. For $d_1 > 60$, the correlation between $x[k]$ and $x[k-d_1]$ is quite small. Note that the impulse response of $H(q)$ (see Figure 5) has most of it energy at the first 60 samples.

Remark 5: In the simulations no stability constraint has been imposed on the filter $A(q)$ of the 2-ch AFC. When the feedback canceller $\hat{F}_0(q)$ is continuously updated during adaptation, the 2-ch AFC has a self-stabilizing feature whereby unstable poles of the closed-loop system $C(q)$ (cf. (13)) and hence also of $\hat{F}(q)=-A^{-1}(q)B(q)$ are migrated back into the unit circle, so that a stability constraint on $A^{-1}(q)$ is not required (cf. Section IV-A). To illustrate this self-stabilizing property, **Figure 8** depicts the maximum amplitude of all poles of $C(q)$ and $A^{-1}(q)$, respectively, as a function of time for the 2-ch AFC with $\lambda=0.9999$, $L_A=5$ and $d_1=5$. The filter length L_A and the delay d_1 were chosen such that the filters $A(q)$ and $B(q)$ of the 2-ch AFC converge to an unstable $A^{-1}(q)$ and unstable closed-loop system $C(q)$ when $\hat{F}_0(q)$ is kept fixed. The upper figure plots the poles for a fixed $\hat{F}_0(q)$. The lower figure considers the case where $\hat{F}_0(q)$ is continuously updated by $-A^{-1}(q)B(q)$, showing that the stability of $C(q)$ and $A^{-1}(q)$ is restored whenever the closed-loop system $C(q)$ becomes unstable.

C. Simulation results: time-varying desired signal $x[k]$

Synthetic desired signal

In practice, the desired signal $x[k]$ will often be a speech signal and hence, highly time-varying. In the first example, we generate a *synthetic speech signal* by passing white, Gaussian noise through a highly time-varying AR-filter, so that the white noise assumption for $w[k]$ is still satisfied. The AR-filter coefficients are derived from the coefficients of an adaptive lattice filter with $\lambda_{\bar{\mathbf{a}}} = 1 - \frac{1}{160}$ operated on a real speech signal. The synthetic signal $x[k]$ is depicted in **Figure 9**. **Figure 10** depicts the misalignment $\zeta(F, \hat{F})$ and the ASG of the different feedback cancellation algorithms. For comparison, the filtered-X algorithm using the average speech model, i.e., an AR model of the long-term average spectrum of the desired signal, is depicted too. As expected, the PEM-AFC offers the best performance for a highly time-varying desired signal $x[k]$. In contrast to the 2-ch AFC and the filtered-X algorithm, the PEM-AFC succeeds in tracking the instantaneous AR-model, resulting in a good feedback path estimate if $d_1 \geq 21$. Even for $15 < d_1 < 21$, the performance of the PEM-AFC for a highly time-varying desired signal is quite good. In the PEM-AFC, the forgetting factor $\lambda_{\hat{\mathbf{f}}}$ of the feedback path estimate $\hat{F}(q)$ is much larger than the forgetting factor $\lambda_{\mathbf{a}}$ of $A(q)$. As a result, the filter $A(q)$ is able to model the fast changes in the speech model $H(q)$ for highly time-varying signals $x[k]$, even when $d_1 < L_A$. Hence, for highly time-varying signals $x[k]$ and $\lambda_{\mathbf{a}} \ll \lambda_{\hat{\mathbf{f}}}$, the identifiability conditions are less crucial than for stationary signals $x[k]$ or $\lambda_{\mathbf{a}} \approx \lambda_{\hat{\mathbf{f}}}$. The 2-ch AFC and filtered-X algorithm provide a less accurate estimate than the PEM-AFC but outperform the CAF if $d \geq 21$. **Figure 11** depicts the filter $A(q)$ obtained by the 2-ch AFC for $d_1 = L_A = 21$ and the inverse of the average PSD of $x[k]$: for sufficiently large d_1, the filter $A(q)$ of the 2-ch AFC is found to converge to the average inverse speech model and hence, the 2-ch AFC approaches the performance of the filtered-X algorithm that uses a model of the long-term average speech spectrum.

Real speech signal

In the second example, $x[k]$ is a *real speech signal*, consisting of sentences spoken by a male speaker. Note that the white noise assumption for $w[k]$ is not completely satisfied anymore: the excitation $w[k]$ of voiced speech segments corresponds to an impulse train rather than to white noise, so that $w[k]$ and $w[k-d]$ may be correlated. Hence, the performance of the adaptive feedback cancellation algorithms is expected to be affected: during voiced segments, the feedback canceller will not only model $H(q)$ and $F(q)$, but will also make an attempt to cancel the impulse train (see also Section III-A). In the 2-ch

AFC, the filter $A(q)$ is seen to converge to the average speech model. The filter $B(q)$, and hence, the feedback canceller $\hat{F}(q) = -A^{-1}(q)B(q)$ then tries to cancel the impulse train excitation. In the PEM-AFC, the fast filter $A(q)$ tries to track the instantaneous speech spectrum: theoretically the filter $A(q)$ ought to notch out all frequencies caused by the impulse train excitation during voiced segments, so that $e_p[k]$ goes to 0 (for any $\hat{F}(q)$). So, adaptation of $\hat{F}(q)$ is effectively performed only during non-voiced speech segments. However, due to the small filter length[8] of $A(q)$ and the limited tracking performance, $e_p[k] \neq 0$ during voiced speech, causing a bias to the feedback path estimate being introduced during voiced speech.

Figure 12(a) depicts the misalignment $\zeta(F, \hat{F})$ of the CAF, the 2-ch AFC and the PEM-AFC as a function of time (expressed in number of samples at f_s) for $d_1 = 30$. The performance of the filtered-X method using the average speech model is depicted too. The CAF has the worst performance among all methods. Initially, the CAF suffers from a huge bias. Due to the time-variability of $x[k]$, the average correlation between $u[k]$ and $x[k]$ decreases for an increasing number of data samples N used in the RLS algorithm. Hence, a slow convergence rate (i.e., a large forgetting factor λ or –in case of LMS– a small step size μ) is beneficial to the CAF at the expense of reduced tracking performance. The 2-ch AFC performs better than the CAF. Compared to the filtered-X algorithm, the 2-ch AFC has a larger number of filter taps, i.e., $L_A + L_B$ taps, and hence, more degrees of freedom to attenuate the frequencies caused by the impulse train excitation. For a smaller $L_A + L_B$ (e.g., $L_A = 11$, $L_B = L_A + L_F - 1$), the 2-ch AFC performs better. The PEM-AFC offers the best performance and convergence rate. The performance of the PEM-AFC can be further improved by inserting uncorrelated noise $r[k]$ at the loudspeaker input. In Figure 12, the performance of the PEM-AFC with $r[k] \neq 0$ is depicted too. The noise $r[k]$ has the long-term average speech spectrum and a level of -20 dB with respect to $G(q)x[k]$. The performance curves of the CAF, the 2-ch AFC and the filtered-X algorithm with $r[k] \neq 0$ almost coincide with the curves for $r[k] = 0$ and are, therefore, omitted. The noise is too low to reduce the bias of the CAF, 2-ch AFC and filtered-X algorithm significantly, but clearly improves the performance of the PEM-AFC.

Figure 12(b) plots the amplitude characteristic of the closed-loop system $1/\left(1 - G(q)(F(q) - \hat{F}(q))\right)$ for the CAF, the 2-ch AFC ($L_A = 11$ and $L_A = 21$) and the PEM-AFC ($r[k] = 0$ and $r[k] \neq 0$). Ideally, the amplitude characteristic should equal 0 dB at all frequencies. The 2-ch AFC outperforms the CAF, but

[8]Note that to cancel the impulse train with period P effectively, the filter $A(q)$ should be able to model the $2L_h$-taps filter $\Pi_{i=1}^{L_h}(1 - e^{j2\pi i \frac{f_0}{f_s}} q^{-1})(1 - e^{-j2\pi i \frac{f_0}{f_s}} q^{-1})$ with $L_h = \left\lfloor \frac{f_s}{2f_0} \right\rfloor$ (see Section III). The pitch frequency f_0 of speech typically lies between 100 Hz and 300 Hz. For $f_s = 16$ kHz, L_A should be between 40 and 160 taps to effectively cancel the impulse train.

exhibits fast fluctuations due to cancellation of the impulse train excitation of voiced speech segments. The PEM-AFC has the smallest amount of signal distortion.

Figure 13 plots the misalignment $\zeta(F, \hat{F})$ and the ASG of the CAF, the 2-ch AFC, the PEM-AFC and the filtered-X algorithm as a function of the delay d_1 for $r[k] = 0$ (dashed-dotted lines) and $r[k] \neq 0$ (dotted lines). The noise has a level of -20 dB with respect to $G(q)x[k]$. In general, the performance measures improve for an increasing delay d_1. For all values of the delay $d_1 \geq 21$, the PEM-AFC outperforms the CAF, the 2-ch AFC and the filtered-X algorithm: on average, the PEM-AFC has a 5 dB larger ASG than the CAF. The 2-ch AFC ($L_A = 21$) outperforms the CAF in misalignment, but often has a worse ASG than the CAF. This is due to the stronger cancellation of the impulse train excitation by the filter $B(q)$ of the 2-ch AFC, which results from the larger number of filter taps (cf. Figure 12(b)). For a smaller $L_A + L_B$ (e.g., $L_A = 11$, $L_B = 60$), the 2-ch AFC was also found to outperform the CAF in ASG. Injection of low-level noise further improves the performance of the PEM-AFC, while the gain in performance of the CAF, the 2-ch AFC and the filtered-X algorithm is negligible.

Music signal

In the last example, $x[k]$ is a *music signal*, consisting of a fragment (25 seconds) of 'Imagine' by John Lennon. **Figure 14** depicts the misalignment $\zeta(F, \hat{F})$ of the CAF, the 2-ch AFC and the PEM-AFC as a function of d_1 for $r[k] = 0$. The performance of the filtered-X method using an average AR model of the music signal is depicted too. The standard CAF suffers from a huge bias, even for $d_1 = 100$. The 2-ch AFC, filtered-X method and PEM-AFC significantly outperform the CAF. Again, the PEM-AFC generally has the best overall performance, although the difference with the filtered-X method that uses the average model of the music signal is small.

VI. CONCLUSIONS

A standard continuous adaptation feedback canceller (CAF) suffers from a large bias if the received sound signal is spectrally colored. To reduce the bias in the feedback path estimate, we proposed adaptive feedback cancellation techniques that are based on closed-loop identification of the feedback path as well as the (auto-regressive) model of the desired signal. In general, both models are not simultaneously identifiable in the closed-loop system at hand. We demonstrated that not only inserting non-linearities or a probe signal, but also adding a delay in the forward path or in the cancellation path can render the system identifiable. The required delay is much smaller than the delay that is needed in the CAF to decorrelate the received sound signal and the loudspeaker signal.

Two recursive procedures for identifying the desired signal model and the feedback path have been derived: a two-channel adaptive feedback canceller (2-ch AFC) as well as a decoupled PEM-AFC. In contrast to the 2-ch AFC, the decoupled PEM-AFC uses a different adaptation for the feedback path and the desired signal model and hence, is preferable for highly non-stationary sound signals.

Simulations demonstrated that both techniques significantly outperform the standard CAF when the identifiability conditions are fulfilled. For a time-varying desired signal $x[k]$, the decoupled PEM-AFC offers the best performance. In the derivation of the identifiability conditions, we assumed that the desired signal is generated by passing white noise through an all-pole filter. If $x[k]$ is a speech signal, the excitation of voiced speech segments corresponds to an impulse train, and hence, the performance of the algorithms is expected to be affected. Simulations showed that the decoupled PEM-AFC has a clear benefit over the CAF also for real speech and music signals. In addition, injection of low-level noise further improves the performance of the PEM-AFC, while the benefit of low-level noise injection to the CAF is negligible.

ACKNOWLEDGMENTS

The authors would like to thank the reviewers for their valuable suggestions and comments.

REFERENCES

[1] J. Hellgren, T. Lunner, and S. Arlinger, "Variations in the feedback of hearing aids," *J. Acoustic. Soc. Am.*, vol. 106, no. 5, pp. 2821–2833, Nov. 1999.

[2] B. Rafaely, M. Roccasalva-Firenze, and E. Payne, "Feedback path variability modeling for robust hearing aids," *J. Acoustic. Soc. Am.*, vol. 107, no. 5, pp. 2665–2673, May 2000.

[3] J. M. Kates, "Room reverberation effects in hearing aid feedback cancellation," *J. Acoustic. Soc. Am.*, vol. 109, no. 1, pp. 367–378, Jan. 2001.

[4] J. M. Kates, *Adaptive feedback cancellation in hearing aids*, chapter 2 in "Adaptive signal processing: Applications to real-world problems" (Benesty, J. and Huang, Y.), pp. 23–55, Springer-Verlag, 2003.

[5] J. A. Maxwell and P. M. Zurek, "Reducing acoustic feedback in hearing aids," *IEEE Trans. Speech, Audio Processing*, vol. 3, no. 4, pp. 304–313, July 1995.

[6] J. E. Greenberg, P. M. Zurek, and M. Brantley, "Evaluation of feedback-reduction algorithms for hearing aids," *J. Acoustic. Soc. Am.*, vol. 108, no. 5, pp. 2366–2376, Nov. 2000.

[7] J. M. Kates, "Feedback cancellation in hearing aids: Results from a computer simulation," *Signal Processing*, vol. 39, no. 3, pp. 553–562, Mar. 1991.

[8] Y. Park, D. Kim, and I. Kim, "An efficient feedback cancellation for multiband compression hearing aids," in *Proc. of 20th Annual Int. Conf. Eng. in Medicine and Biology Soc.*, 1998, vol. 5, pp. 2706–2709.

[9] S. Thipphayathetthana and C. Chinrungrueng, "Variable step-size of the least-mean-square algorithm for reducing acoustic feedback in hearing aids," in *IEEE Asi-Pacific Conf. on Circuits and Systems*, 2000, pp. 407–410.

[10] M. G. Siqueira and A. Alwan, "Steady-state analysis of continuous adaptation in acoustic feedback reduction systems for hearing-aids," *IEEE Trans. Speech, Audio Processing*, vol. 8, no. 4, pp. 443–453, July 2000.

[11] C. P. Janse and P. A. A. Timmermans, "Signal amplifier system with improved echo cancellation," U.S. patent, US 5748751, 1998.

[12] H. A. L. Joson, F. Asano, Y. Suzuki, and S. Toshio, "Adaptive feedback cancellation with frequency compression for hearing aids," *J. Acoustic. Soc. Am.*, vol. 94, no. 6, pp. 3248–3254, Dec. 1993.

[13] J. L. Nielsen and U. P. Svensson, "Performance of some linear time-varying systems in control of acoustic feedback," *J. Acoustic. Soc. Am.*, vol. 1, no. 106, pp. 240–254, July 1999.

[14] A. M. Engebretson and M. F. George, "Properties of an adaptive feedback equalization algorithm," *J. Rehab. Res. Dev.*, vol. 30, no. 1, pp. 8–16, 1993.

[15] H. R. Skovgaard, "Hearing aid compensating for acoustic feedback," US Patent, US 5680467, 1997.

[16] J. M. Kates, "Constrained adaptation for feedback cancellation in hearing aids," *J. Acoustic. Soc. Am.*, vol. 106, no. 2, pp. 1010–1019, Aug. 1999.

[17] H.-F. Chi, S. X. Goa, S. D. Soli, and A. Alwan, "Band-limited feedback cancellation with a modified filtered-X LMS algorithm for hearing aids," *Speech Communication*, vol. 39, no. 1-2, pp. 147–161, Jan. 2003.

[18] J. Nielsen and M. Ekelid, "Feedback cancellation with low frequency input," WO Patent, WO 01/06812 A1, 2001.

[19] R. Leber and W. Schaub, "Circuit and method for the adaptive suppression of an acoustic feedback," U.S. patent, US 6611600, 2003.

[20] J. Hellgren, "Analysis of feedback cancellation in hearing aids with filtered-X LMS and the direct method of closed loop identification," *IEEE Trans. Speech, Audio Processing*, vol. 10, no. 2, pp. 119–131, Feb. 2002.

[21] J. Hellgren and U. Forssell, "Bias of feedback cancellation algorithms in hearing aids based on direct closed loop identification," *IEEE Trans. Speech, Audio Processing*, vol. 9, no. 7, pp. 906–913, Nov. 2001.

[22] N. A. Shusina and B. Rafaely, "Feedback cancellation in hearing aids based on indirect close-loop identification," in *Proc. IEEE Benelux Signal Processing Symposium (SPS)*, Leuven, Belgium, Mar. 2002, pp. 177–180.

[23] U. Forssell, *Closed-loop identification – methods, theory and applications*, Ph.D. thesis, Linköping Universitet, Linköping, Sweden, 1999.

[24] U. Forssell and L. Ljung, "Closed-loop identification revisited," *Automatica*, vol. 35, pp. 1215–1241, 1999.

[25] J. R. Deller, J. G. Proakis, and J. H. L. Hansen, *Discrete-Time Processing of Speech Signals*, Macmillan Publishing Company, Englewood Cliffs, New Jersey, 1993.

[26] M. A. Stone and B. C. J. Moore, "Tolerable hearing aid delays. I. estimation of limits imposed by the auditory path alone using simulated hearing losses," *Ear and Hearing*, vol. 20, no. 3, pp. 182–191, 1999.

[27] S. Laugesen, K. V. Hansen, and J. Hellgren, "Acceptable delays in hearing aids and implications for feedback cancellation," *J. Acoustic. Soc. Am.*, vol. 105, no. 2, pp. 1211–1212, 1999.

[28] M. N. Murthi and B. D. Rao, "All-pole modeling of speech based on minimum variance distortionless response spectrum," vol. 8, no. 3, pp. 221–239, May 2000.

[29] J. E. Greenberg, "Modified LMS algorithms for speech processing with an adaptive noise canceller," *IEEE Trans. Speech, Audio Processing*, vol. 6, no. 4, pp. 338–350, July 1998.

[30] S. Haykin, *Adaptive filter theory*, Information and system sciences series. Prentice Hall, Englewood Cliffs, New Jersey, 4th edition edition, 2001.

[31] J. J. Shynk, "Adaptive IIR filtering," *IEEE ASSP Magazine*, vol. 6, no. 2, pp. 4–21, Apr. 1989.

[32] L. Ljung and T. Söderström, *Theory and Practice of Recursive Identification.*, MIT Press, Cambridge, MA, 1983.

[33] J. Makhoul, "Stable and efficient lattice methods for linear prediction," *IEEE Trans. Acoust., Speech, and Signal Processing*, vol. 25, no. 5, pp. 423–428, Oct. 1977.

[34] M. Mboup, M. Bonnet, and N. Bershad, "LMS coupled adaptive prediction and system identification: a statistical model and transient mean analysis," *IEEE Trans. Signal Processing*, vol. 42, no. 10, pp. 2607–2615, Oct. 1994.

[35] M. Bouchard and S. Quednau, "Multi-channel recursive-least-squares algorithms and fast-transversal-filter algorithms for active noise control and sound reproduction systems," *IEEE Trans. Speech, Audio Processing*, vol. 8, no. 5, pp. 606–618, Sept. 2000.

[36] A. Spriet, *Adaptive filtering techniques for noise reduction and acoustic feedback cancellation in hearing aids*, Ph.D. thesis, Faculty of Engineering, K.U. Leuven, Leuven, Belgium, Sept. 2004, available as Tech. Rep. ESAT-SISTA/TR 04-137.

[37] A. Spriet, I. Proudler, M. Moonen, J. Wouters, "An Instrumental variable method for adaptive feedback cancellation in hearing aid," in *Proc. International Conference on Acoustics, Speech, and Signal Processing (ICASSP 2005)*, Philadelphia, PA, USA, March 2005, vol. 3, pp. 129-132.



Ann Spriet (S'01) was born in Izegem, Belgium, in 1976. She received the Electrical Engineering degree and the Ph.D. degree in applied sciences from the Katholieke Universiteit Leuven, Leuven, Belgium, in 1999 and 2004, respectively. From 1999 until 2003, she was a Research Assistant of the Fonds voor Wetenschappelijk Onderzoek - Vlaanderen. Currently, she is a postdoctoral researcher at the Electrical Engineering Department (ESAT) of the Katholieke Universiteit Leuven, in the framework of a collaboration with Katholieke Universiteit Leuven - Laboratory Experimental ORL. Her research interests are in digital signal processing for speech enhancement in hearing aids and cochlear implants. She received the 2001 Lapperre Award, a Best Student Paper Award at the International Workshop on Acousctic Echo and Noise Control in 2003 and a Best Student Paper Award at the International Conference on Acoustics, Speech, and Signal Processing in 2005.



Ian Proudler received a first class honours degree (Physics) from Oxford University in 1978 and his PhD in Digital Signal Processing from the University of Cambridge in 1984. In between he spent two years doing R&D work in Industry. He remained at the Cambridge University Engineering department until 1986 as a Post. Doc. working on finite precision effects in digital filters. He joined QinetiQ (then RSRE and subsequently DERA) in 1986 and started work in the field of adaptive digital signal processing with particular emphasis on least squares minimisation algorithms and architectures. He was awarded the 1992 John Benjamin Memorial Prize for his discovery of the QRD-based least squares lattice algorithm. He received the award again 2002 for work on the novel KaGE fast least squares algorithm. He is the 2002 recipient of the IEE J.J. Thomson Medal "for outstanding work in electronics theory, practice, development or manufacture." He has been the Principal Researcher or a task leader on several advanced research projects. He was elected a QinetiQ Fellow in 1998. He has published some 60+ research papers and made contributions to 4 text books. He has been on the organising committee of several international conferences. He is an Honorary Editor for IEE Proceedings: Radar, Sonar and Navigation and a visiting Professor at the Department of Electronic Engineering, King's College, London.



Marc Moonen (M'94) received the Electrical Engineering degree and the Ph.D. degree in applied sciences from the Katholieke Universiteit Leuven, Leuven, Belgium, in 1986 and 1990, respectively. Since 2000 he has been an Associate Professor with the Electrical Engineering Department, Katholieke Universiteit Leuven, where he is currently heading a research team of sixteen Ph.D. candidates and postdocs, working in the area of signal processing for digital communications, wireless communications, DSL, and audio signal processing. Dr. Moonen received the 1994 KU Leuven Research Council Award, the 1997 Alcatel Bell (Belgium) Award (with P. Vandaele) and was a 1997 "Laureate of the Belgium Royal Academy of Science." He was Chairman of the IEEE Benelux Signal Processing Chapter (1998-2002), and is currently a EURASIP AdCom Member (European Association for Signal, Speech, and Signal Processing, 2000). He is Editor-in Chief for the *EURASIP Journal on Applied Signal Processing* (2003), and a member of the editorial board of *Integration, the VLSI Journal, IEEE Transactions on Circuits and Systems II, EURASIP Journal on Wireless Communications and Networking, and IEEE Signal Processing Magazine*.



Jan Wouters was born in Leuven, Belgium, in 1960. He received the physics degree and the Ph.D. degree in sciences / physics from the Katholieke Universiteit Leuven, Leuven, Belgium, in 1982 and 1989, respectively. From 1989 till 1992 he has been a Research Fellow with the Belgian NFWO (National Fund for Scientific Research) at the Institute of Nuclear Physics (UCL Louvain-la-Neuve and KU Leuven) and at NASA Goddard Space Flight Center (USA). From 1993 he is a Professor at the Neurosciences Department of the Katholieke Universiteit Leuven. His research activities are about audiology and the auditory system, signal processing for cochlear implants and hearing aids. Dr. Wouters received in 1989 an Award of the Flemish Ministry, in 1992 a Fullbright Award and a NATO Research Fellowship, the 1996 Flemish VVL Speech therapy - Audiology Award. He is member of the International Collegium for Rehabilitative Audiology, a Board Member of the NAG (Dutch Acoustical Society) and responsible for the Lab. Exp. ORL, author of 75 articles in international peer-review journals, reviewer for several international journals.

LIST OF FIGURES

1 Adaptive feedback cancellation algorithm with continuous adaptation (CAF). 30

2 Direct closed-loop identification of the feedback path $F(q)$ with the PEM. 30

3 Two-channel identification method. 30

4 PEM-AFC 31

5 Frequency characteristic of the feedback path $F(q)$. 31

6 Impulse response of all-pole filter $H(q)$. 31

7 Misalignment $\zeta(F, \hat{F})$ of the CAF, the 2-ch AFC, the PEM-AFC and the filtered-X algorithm as a function of the delay d_1. 32

8 Maximum amplitude of all poles of $C(q)$ and $A^{-1}(q)$ as a function of time. The upper figure considers the case where $\hat{F}_0(q)$ is kept fixed. The lower figure considers the case where $\hat{F}_0(q)$ is continuously updated. 32

9 Synthetic speech signal $x[k]$. 33

10 Misalignment $\zeta(F, \hat{F})$ (a) and ASG (b) of CAF, 2-ch AFC, PEM-AFC and Filtered-X for a highly time-varying synthetic speech signal $x[k]$. 33

11 Comparison between the amplitude characteristic of the filter $A(q)$ of the 2-ch AFC and the inverse of the average PSD of $x[k]$. 33

12 (a) Misalignment as a function of time for a real speech signal $x[k]$. (b) Amplitude characteristic of the closed loop response $1/(1 - G(q)(F(q) - \hat{F}(q)))$ of the CAF, the 2-ch AFC and the PEM-AFC. 34

14 Misalignment $\zeta(F, \hat{F})$ of the CAF, the 2-ch AFC, the PEM-AFC and the filtered-X algorithm as a function of the delay d_1 for a music signal $x[k]$. 34

13 Misalignment $\zeta(F, \hat{F})$ (a) and ASG (b) of the CAF, the 2-ch AFC, the PEM-AFC ($L_A = 21$) and the filtered-X algorithm for a real speech signal $x[k]$. The dashed-dotted lines correspond to $r[k] = 0$. The dotted lines correspond to $r[k] \neq 0$. 35

LIST OF ALGORITHMS

1 Burg lattice algorithm. 35

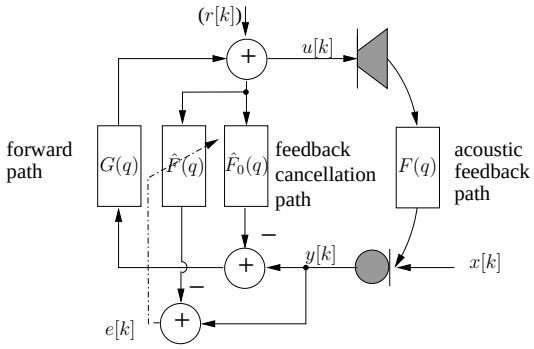

Fig. 1. Adaptive feedback cancellation algorithm with continuous adaptation (CAF).

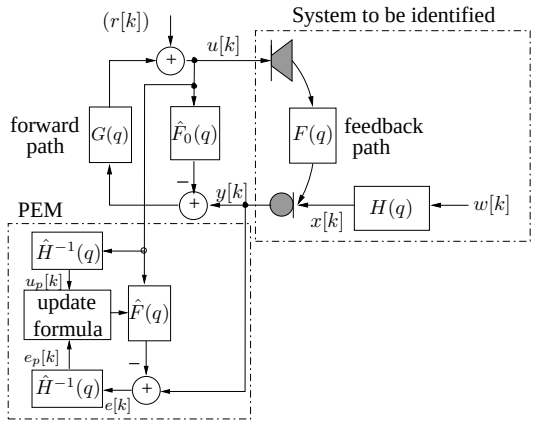

Fig. 2. Direct closed-loop identification of the feedback path $F(q)$ with the PEM.

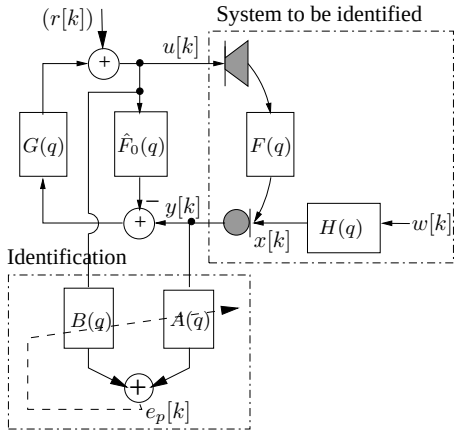

Fig. 3. Two-channel identification method.

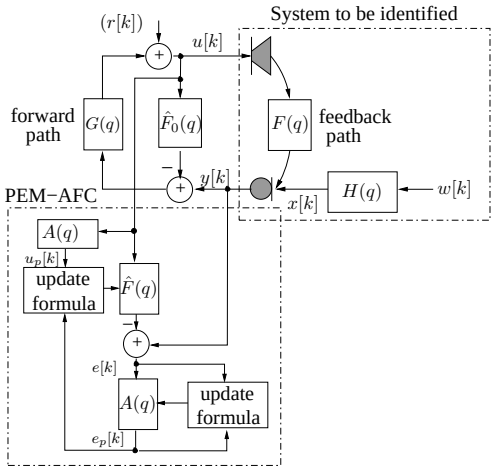

Fig. 4. PEM-AFC

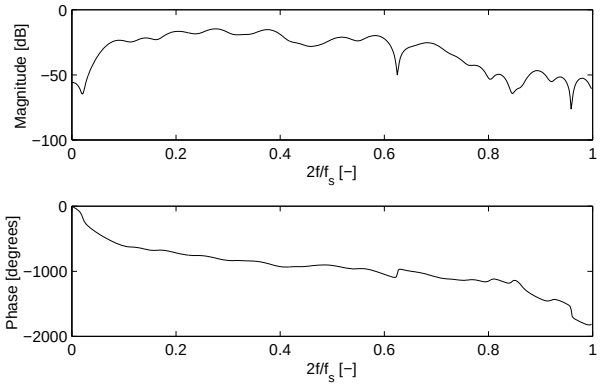

Fig. 5. Frequency characteristic of the feedback path $F(q)$.

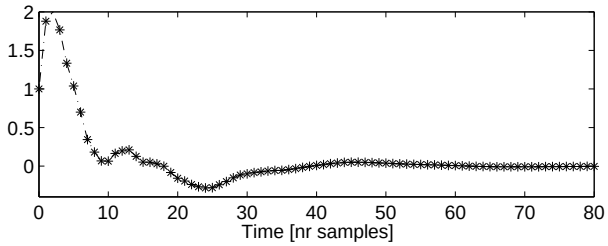

Fig. 6. Impulse response of all-pole filter $H(q)$.

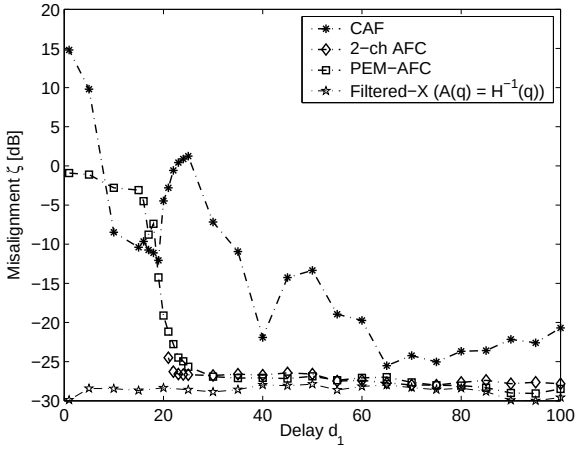

Fig. 7. Misalignment $\zeta(F, \hat{F})$ of the CAF, the 2-ch AFC, the PEM-AFC and the filtered-X algorithm as a function of the delay d_1.

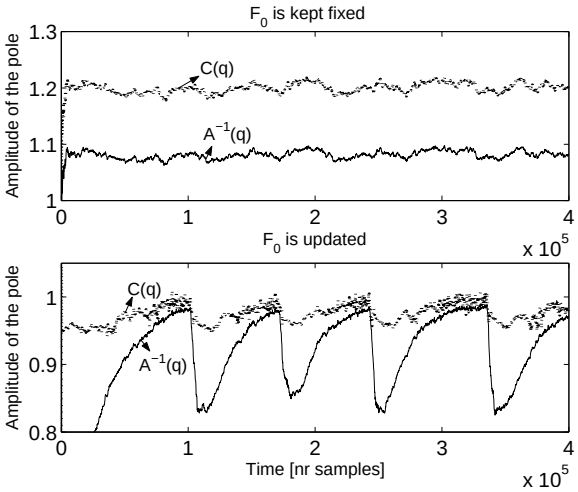

Fig. 8. Maximum amplitude of all poles of $C(q)$ and $A^{-1}(q)$ as a function of time. The upper figure considers the case where $\hat{F}_0(q)$ is kept fixed. The lower figure considers the case where $\hat{F}_0(q)$ is continuously updated.

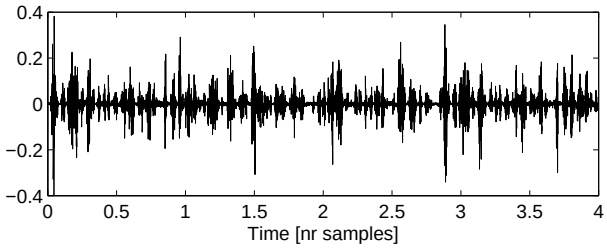

Fig. 9. Synthetic speech signal $x[k]$.

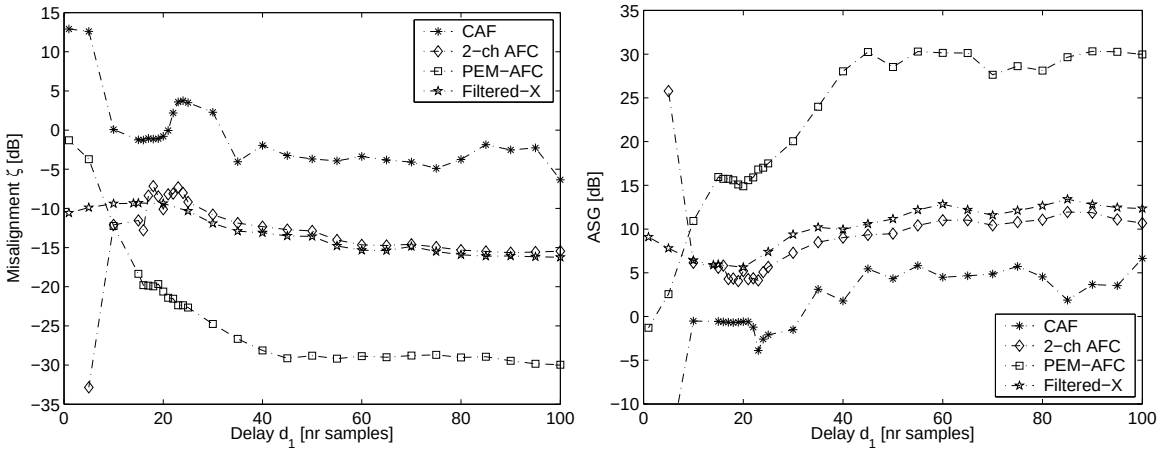

(a) (b)

Fig. 10. Misalignment $\zeta(F, \hat{F})$ (a) and ASG (b) of CAF, 2-ch AFC, PEM-AFC and Filtered-X for a highly time-varying synthetic speech signal $x[k]$.

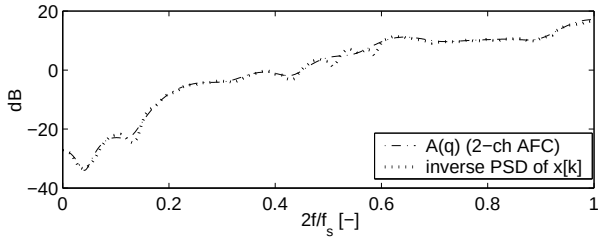

Fig. 11. Comparison between the amplitude characteristic of the filter $A(q)$ of the 2-ch AFC and the inverse of the average PSD of $x[k]$.

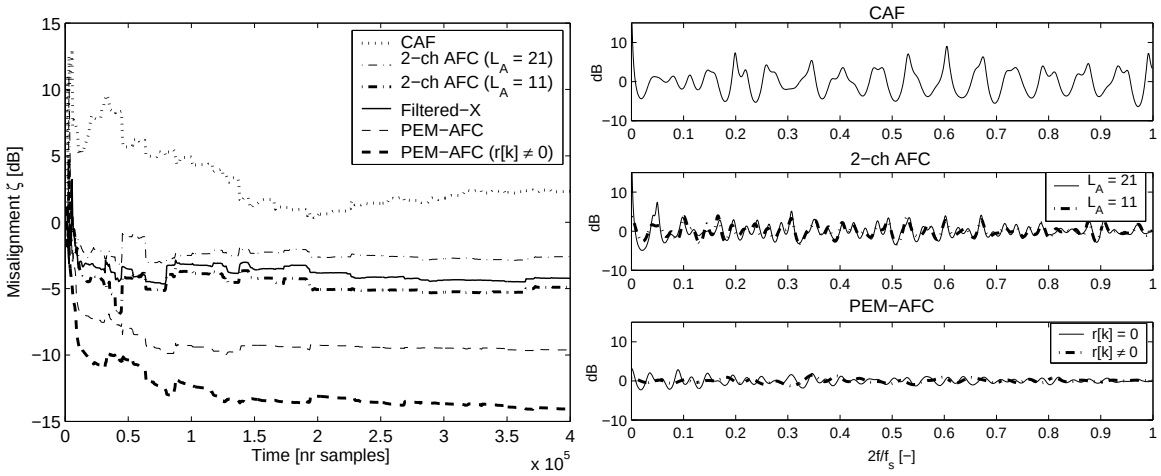

(a) (b)

Fig. 12. (a) Misalignment as a function of time for a real speech signal $x[k]$. (b) Amplitude characteristic of the closed loop response $1/(1 - G(q)(F(q) - \hat{F}(q)))$ of the CAF, the 2-ch AFC and the PEM-AFC.

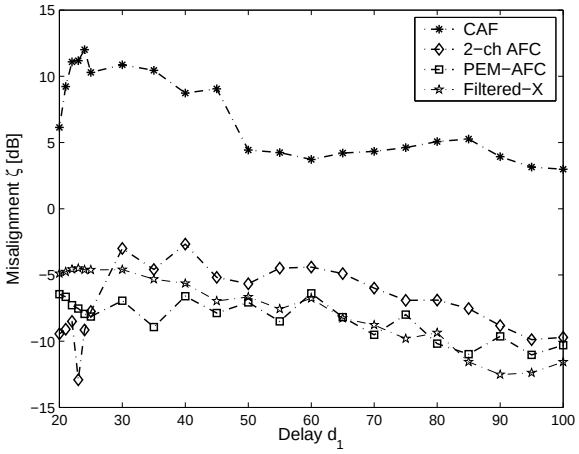

Fig. 14. Misalignment $\zeta(F, \hat{F})$ of the CAF, the 2-ch AFC, the PEM-AFC and the filtered-X algorithm as a function of the delay d_1 for a music signal $x[k]$.

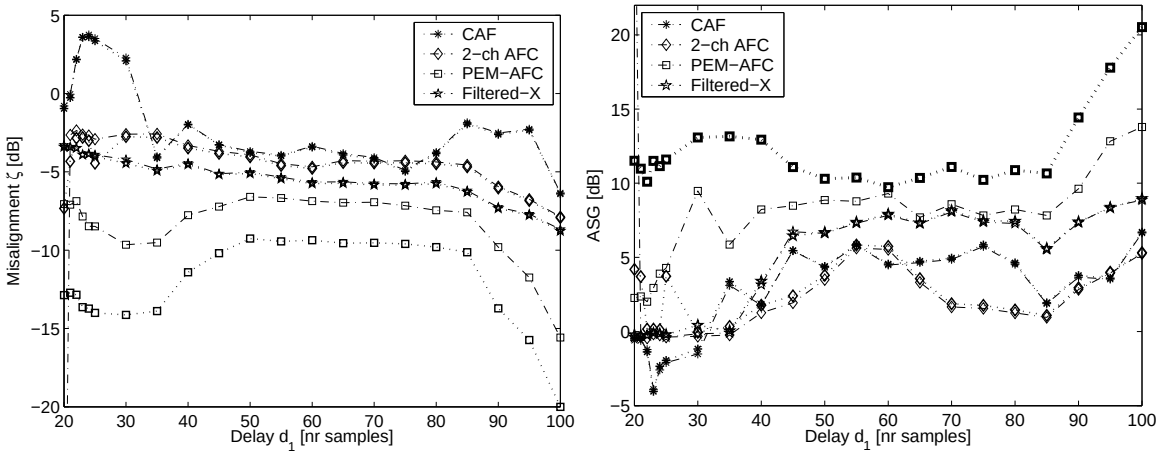

(a) (b)

Fig. 13. Misalignment $\zeta(F, \hat{F})$ (a) and ASG (b) of the CAF, the 2-ch AFC, the PEM-AFC ($L_A = 21$) and the filtered-X algorithm for a real speech signal $x[k]$. The dashed-dotted lines correspond to $r[k] = 0$. The dotted lines correspond to $r[k] \neq 0$.

Algorithm 1 Burg lattice algorithm.

$f_0[k] = \epsilon[k] = y[k] - \hat{\mathbf{f}}[k-1]\mathbf{u}[k]$;

$b_0[k] = \epsilon[k]$;

For $i = 1, \cdots, L_A - 1$:

$d_i[k] = \lambda_{\bar{\mathbf{a}}} d_i[k-1] + (1 - \lambda_{\bar{\mathbf{a}}}) \left[f_{i-1}^2[k] + b_{i-1}^2[k-1] \right]$

$n_i[k] = \lambda_{\bar{\mathbf{a}}} n_i[k-1] + (1 - \lambda_{\bar{\mathbf{a}}})(-2) f_{i-1}[k] b_{i-1}[k-1]$

$\kappa_i[k] = \frac{n_i[k]}{d_i[k]}$

$f_i[k] = f_{i-1}[k] + \kappa_i[k] b_{i-1}[k-1]$

$b_i[k] = \kappa_i[k] f_{i-1}[k] + b_{i-1}[k-1]$